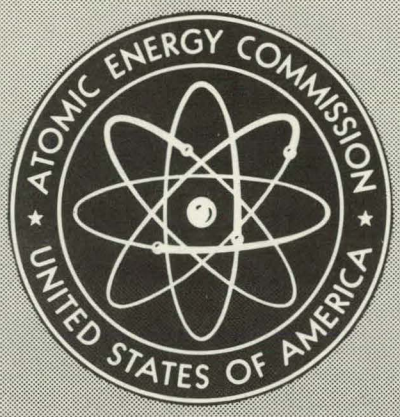

ORNL-3130

BARYTES CONCRETE FOR RADIATION SHIELDING: MIX CRITERIA AND ATTENUATION CHARACTERISTICS

By
William J. Grantham, Jr.

July 25, 1961

Oak Ridge National Laboratory
Oak Ridge, Tennessee

UNITED STATES ATOMIC ENERGY COMMISSION • DIVISION OF TECHNICAL INFORMATION

DISCLAIMER

This report was prepared as an account of work sponsored by an agency of the United States Government. Neither the United States Government nor any agency Thereof, nor any of their employees, makes any warranty, express or implied, or assumes any legal liability or responsibility for the accuracy, completeness, or usefulness of any information, apparatus, product, or process disclosed, or represents that its use would not infringe privately owned rights. Reference herein to any specific commercial product, process, or service by trade name, trademark, manufacturer, or otherwise does not necessarily constitute or imply its endorsement, recommendation, or favoring by the United States Government or any agency thereof. The views and opinions of authors expressed herein do not necessarily state or reflect those of the United States Government or any agency thereof.

DISCLAIMER

Portions of this document may be illegible in electronic image products. Images are produced from the best available original document.

LEGAL NOTICE

This report was prepared as an account of Government sponsored work. Neither the United States, nor the Commission, nor any person acting on behalf of the Commission:

A. Makes any warranty or representation, expressed or implied, with respect to the accuracy, completeness, or usefulness of the information contained in this report, or that the use of any information, apparatus, method, or process disclosed in this report may not infringe privately owned rights; or

B. Assumes any liabilities with respect to the use of, or for damages resulting from the use of any information, apparatus, method, or process disclosed in this report.

As used in the above, "person acting on behalf of the Commission" includes any employee or contractor of the Commission, or employee of such contractor, to the extent that such employee or contractor of the Commission, or employee of such contractor prepares, disseminates, or provides access to, any information pursuant to his employment or contract with the Commission, or his employment with such contractor.

This report has been reproduced directly from the best available copy.

Printed in USA. Price $1.50. Available from the Office of Technical Services, Department of Commerce, Washington 25, D. C.

USAEC Division of Technical Information Extension, Oak Ridge, Tennessee

ORNL- 3130

Contract No. W-7405-eng-26

Neutron Physics Division

BARYTES CONCRETE FOR RADIATION SHIELDING: MIX CRITERIA AND ATTENUATION CHARACTERISTICS

William J. Grantham, Jr.

Date Issued

July 25, 1961

OAK RIDGE NATIONAL LABORATORY
Oak Ridge, Tennessee
operated by
UNION CARBIDE CORPORATION
for the
U.S. ATOMIC ENERGY COMMISSION

THIS PAGE

WAS INTENTIONALLY

LEFT BLANK

PREFACE

The widespread use of concrete as a radiation shielding material has established a need for mix design criteria primarily oriented toward shielding problems. Because increases in density of a shield, per se, result in increased attenuation efficiency for both neutrons and gamma rays, and because elements of high atomic number attenuate gamma rays more efficiently than those of low atomic number, heavy-mineral aggregates are frequently employed to increase the density of shield concrete. If, in addition, the heavy aggregates are randomly packed more efficiently through proper gradation control, the increase in density will further increase the gamma-ray attenuation efficiency and, depending upon the characteristics of the aggregate, may improve neutron attenuation as well. In the first portion of this report, the effects of aggregate gradation and proportions upon concrete density are examined, and criteria for efficient mix proportioning of concretes to be used in shielding are proposed.

In the design of radiation shields for portable, temporary, or remote reactor installations, it may be desirable to discount the structural significance of concrete, and let the shield consist of the dry components alone, or, in the extreme, of the dry aggregates alone. In other instances, a concrete shield may be exposed to temperatures in excess of 100°C, driving off all water except the 1 or 2 per cent by weight firmly held by hydration.[1] The lack of or disappearance of water would obviously decrease the effectiveness of the shield simply as a result of density change, and in addition decrease the ability of the shield to attenuate fast neutrons, since water is highly effective in moderating energetic neutrons to thermal energies where absorption is more probable. In an effort to quantitatively evaluate these

---

1. R. Wilson and F. L. Martin, "Water Retained in Hardened Cement Paste," J. Am. Concrete Inst., Proc., Vol. 31 (1935).

effects, a study has been made of the attenuation properties of barytes aggregate alone, barytes aggregate plus portland cement (a "waterless concrete"), and finally, for comparison, the attenuation properties of barytes concrete. This comprises the second portion of this report.

ABSTRACT

Concrete mix design criteria, based on existing theories of proportioning and specifically oriented toward the solution of radiation shielding problems, have been developed. Effects of aggregate gradation, cement-to-aggregate ratio, and water content were examined.

A barytes concrete, designed according to these criteria, has been thoroughly investigated in the Lid Tank Shielding Facility of Oak Ridge National Laboratory. Relative effectivenesses of dry aggregates, aggregates plus cement, and cured concrete have been compared through thermal-neutron flux, fast-neutron dose, and gamma-ray dose measurements behind slab configurations. Attenuation was measured for the aggregate, the aggregate plus cement, and for the barytes concrete. Comparison with attenuations calculated on the basis of removal cross sections for the measured chemical compositions showed satisfactory agreement.

TABLE OF CONTENTS

I. EFFICIENT PROPORTIONING OF CONCRETE MIXES

Introduction

Present practices with regard to proportioning of concrete mixes were in general developed over 30 years ago. At that time high density, of itself, was not of particular concern. Of the several existing theories, the most applicable were developed by Abrams[2] and by Talbot and Richart.[3] The principles and procedures described by these men are combined to develop the maximum density theory presented here.

The amount of mixing water needed to make workable concrete is always far in excess of the amount required to hydrate the cement. The excess water displaces materials of higher density and therefore significantly lowers the density of the concrete. By efficient proportioning and gradation control, the amount of mixing water can be held to a minimum, resulting in increases in concrete density. The amount of mixing water needed to make a mix workable is partially controlled by the amount of cement in the mix and partially by the fineness gradation of the aggregate. Generally speaking, the leaner the mix (low cement content) the smaller the amount of mixing water needed for workability; also, the coarser the gradation (within limits) the smaller the amount of mixing water needed. These two axioms do not work together, however. Lean mixes require fine gradations in order to maintain plasticity. (A mix is workable only when it has plasticity, i.e., will not crumble or separate at the desired fluidity.) An ideal mix with regard to maximum density is consequently one in which the least practicable amount of cement is used and the aggregate gradation is as coarse as workability will permit. This thesis presumes that the aggregate specific gravity is greater than that of the cement. Otherwise, some optimization may be necessary.

---

2. D. A. Abrams, Design of Concrete Mixes, Structural Materials Research Laboratory Bulletin 1, Lewis Institute (1921).
3. A. N. Talbot and F. E. Richart, The Strength of Concrete - Its Relation to Cement, Aggregate, and Water, Engineering Experiment Station Bulletin 137, University of Illinois (1923).

A numerical procedure developed by Abrams[2] for evaluating a gradation places emphasis on the distribution of particle sizes. Abrams designated this evaluation as fineness modulus and computed it as the summation of the cumulative fractions retained above particular sieve sizes -- U.S. Standard sizes Nos. 100, 50, 30, 16, 8, and 4, 3/8 in., 3/4 in., 1-1/2 in., 3 in., and up, by ratios of 2:1. This emphasis on particle-size distribution is so well directed that any two gradations with the same fineness modulus require approximately the same amount of mixing water. In the present study, several fineness moduli were estimated for various volumetric ratios of cement to aggregate. Since maximum permissible fineness modulus is also a function of maximum aggregate size, the investigation included a study of the following frequently used maximum sizes: 3/8 in., 3/4 in., and 1-1/2 in. In order to project the data into mix proportioning information, corresponding maximum amounts of mixing water were also estimated.

Although it is known that naturally rounded aggregates require less mixing water than crushed aggregates, it is anticipated that aggregates for shielding purposes will in general be crushed. Since crushed barytes aggregates are frequently used in concrete shields, they were chosen for this study. Within reasonable limits, the results should, however, be applicable to other crushed aggregates. If naturally rounded aggregates are to be used, mixing water estimates, and therefore density estimates, should be conservative.

Laboratory Procedure

Both the coarse and fine aggregates were separated into fractional sizes so that they might be recombined according to desired gradations. It is believed that material finer than No. 100 sieve size, while aiding workability, increases mixing water demand;[4,5] therefore, all material passing the No. 100 sieve was discarded.

---

4. C. T. Kennedy, "The Design and Control of Concrete Mixes," J. Am. Concrete Inst., Proc., Vol. 36 (1935).
5. D. A. Abrams, "Discussion of 'The Design and Control of Concrete Mixes' by C. T. Kennedy," J. Am. Concrete Inst., Proc., Vol. 36 (1935).

For each of the maximum sizes, 3/8 in., 3/4 in., and 1-1/2 in., several cement-to-aggregate volume ratios were investigated. For each ratio, one, two, or three trial fineness moduli were selected from a table of maximum permissible fineness moduli given by Abrams.[2] The fractional sizes were then recombined according to those selected fineness moduli. Table 1 indicates the number of trial batches prepared for each condition.

Table 1. Number of Trial Batches Prepared, for Each Aggregate Size

Maximum Size of Aggregate (in.)	Cement-to-Aggregate Volume Ratio						
	1:2	1:3	1:5	1:8	1:12	1:16	Total
3/8	3	3	3	3	3	1	16
3/4	3	3	3	3	3	1	16
1-1/2	2		2		2	1	7

The two extreme gradation curves for 1-1/2 in. maximum size are shown in Fig. 1. By disregarding on each curve all material coarser than 3/4 in., and normalizing the curves to 100% passing, these two curves can be made to indicate the two extreme fineness moduli for the 3/4 in. maximum size. The same is true for the 3/8 in. maximum size, etc.

For purposes of proportioning, the following aggregate characteristics were determined:[6]

(1) saturated-surface-dry specific gravity: 4.13,

(2) saturated-surface-dry water content: 0.85% by weight of oven-dry,

(3) room-dry water content: 0.17% by weight of oven-dry,

(4) ratio of room-dry weight to saturated-surface-dry weight: 0.9933.

6. It should be noted that the aggregates used in this portion of the study were mined at Cartersville, Georgia. Those used in the second portion of the study were mined at Sweetwater, Tennessee.

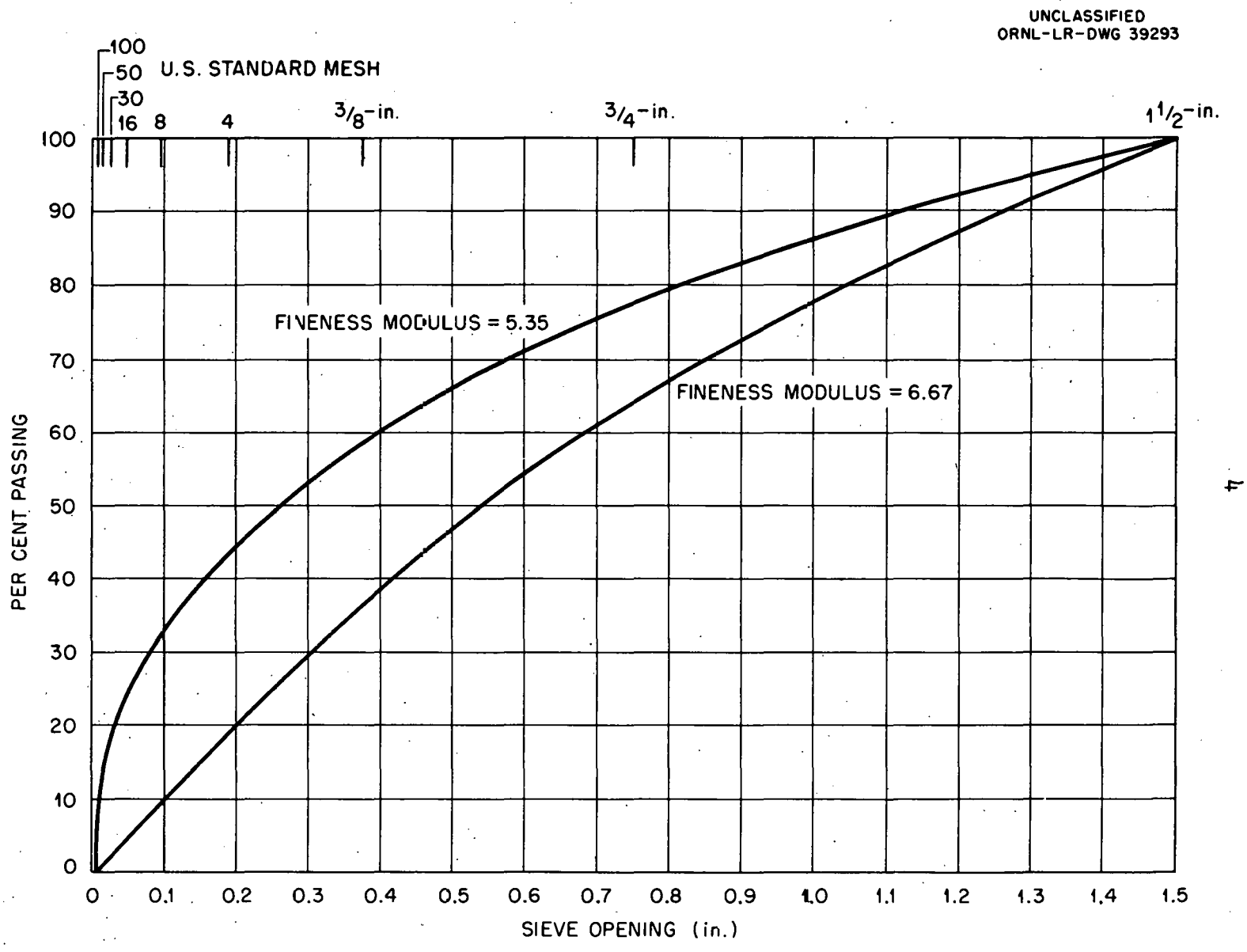

Fig. 1. Gradation Curves.

A generally accepted value, 3.15, was used for the specific gravity of cement, and 1.0 was assumed for the specific gravity of water.

The mortar-voids technique of Talbot and Richart[3] was employed to estimate the amount of mixing water required to obtain minimum actual volumes, that is, the absolute volume, the total volume of solids, plus void volume. The mixer employed was a small rotating-barrel type of approximately 0.5 ft^3 capacity.

For each trial batch, Type-I Portland cement and saturated-surface-dry, barytes aggregates were proportioned so as to obtain a 3000-cm^3 total volume of solids. The initial 3000 cm^3 was placed in the mixer and allowed to mix thoroughly. Water was then added in increments of 100 cm^3 until the mix began to show plasticity. Thereafter, water was added in increments of 50 cm^3, and the unit weight of the concrete determined after each increment. For unit weight determinations, the concrete was compacted into a 0.1 ft^3 container with the aid of a vibration table. Vibration gave results that were more consistent than those obtainable by conventional rodding, and, moreover, the effects of vibration were good observational criteria for estimating workability. Because of the time delay in adding water by increments and in unit weight determinations, total mixing time was usually 50 to 60 minutes. Figure 2 is a typical illustration of the results obtained. The workability terms of Fig. 2 are defined as follows:

(1) Dry: too harsh to be considered workable, even in the vaguest sense.

(2) Stiff: workable, provided vibration technique is employed.

(3) Loose: workable, when vibration technique is not employed.

(4) Watery: too fluid to be considered workable, even in the vaguest sense.

It is important to note that although an optimum in workability may occur as a transition from stiff to loose, the optimum will not exist for each and every mix.

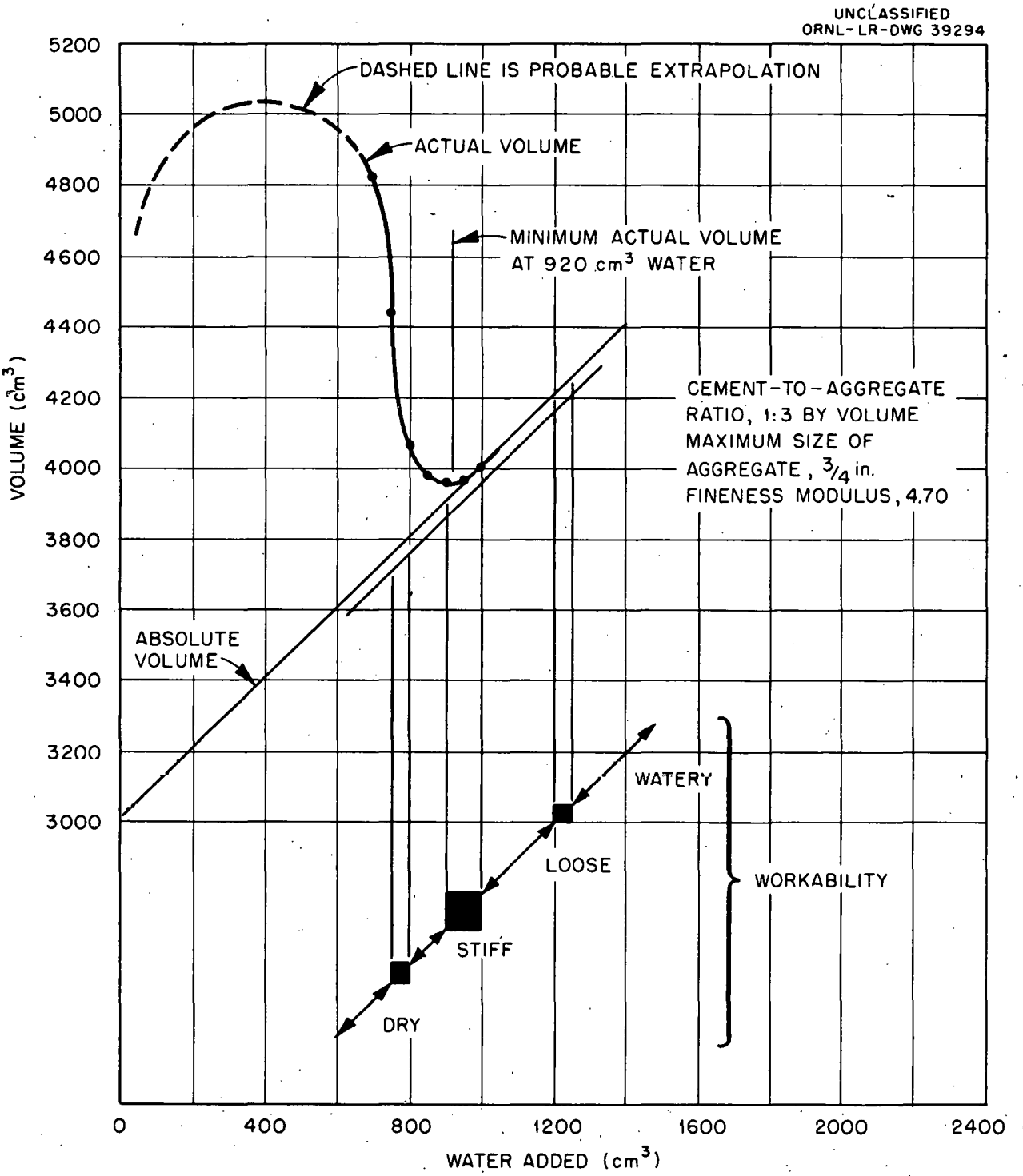

Fig. 2. Concrete Volume vs. Water Added.

The procedure used to estimate ideal fineness moduli and corresponding required minimum amounts of mixing water is demonstrated by the example shown in Fig. 3.

The center-most vertical region, the shaded portion of the figure, indicates concrete that is ideally workable; the two adjacent vertical regions indicate concrete that is only conditionally workable.

Test Results

The results of the gradation studies are shown in Fig. 4. The curves show maximum, recommended fineness modulus as a function of cement-to-aggregate volume ratio. The interrelation of the curves is more clearly shown by the logarithmic plot of Fig. 5, which is a cross plot of values from the curves of Fig. 4. Figure 5 should permit easier and more accurate interpolations and extrapolations. Several seemingly representative curves were fitted to the data in Fig. 4 before a satisfactory pattern appeared in Fig. 5. The curves shown in each represent what seems to be a satisfactory resolution.

Mixing water requirements per 3000 cm^3 of cement and aggregate are shown in Fig. 6, in which the curves represent minimum mixing-water requirements for the corresponding batches of Fig. 4. The curves of Fig. 6 were used to plot the water-cement ratio curves of Fig. 7, which can be used to predict anticipated concrete strengths. Average concrete strength as a function of water-cement ratio is also shown in Fig. 7. It should be noted that these are accurate only to ± 12 per cent.[7] In order to facilitate interpolations and extrapolations, a logarithmic plot of water-cement ratio versus maximum size of aggregate is given in Fig. 8. A fitting adjustment similar to that used for the fineness modulus results was used on the water content results. The

---

7. Portland Cement Association, Design and Control of Concrete Mixtures (Chicago: By the author, 1952).

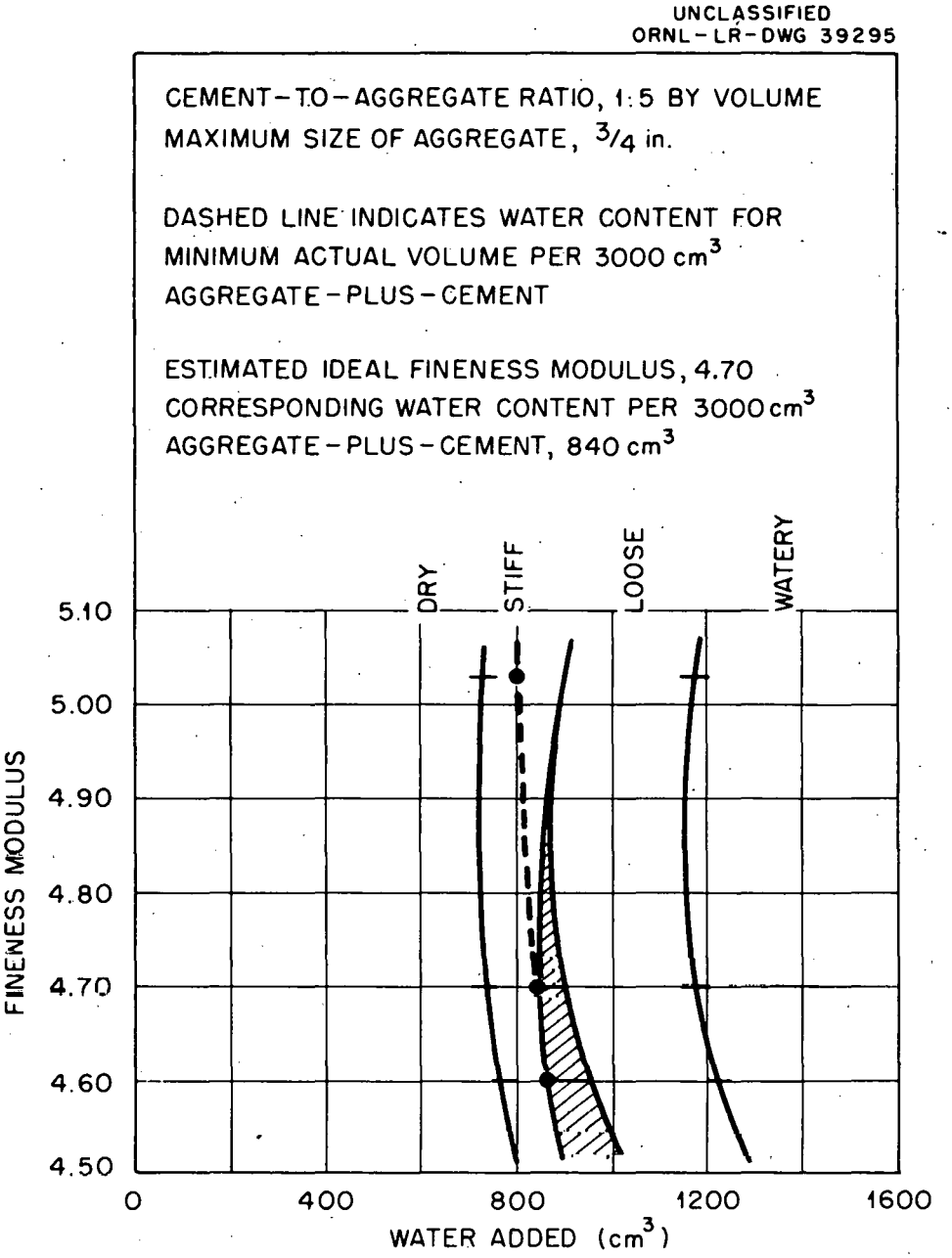

Fig. 3. Workability as a Function of Fineness Modulus.

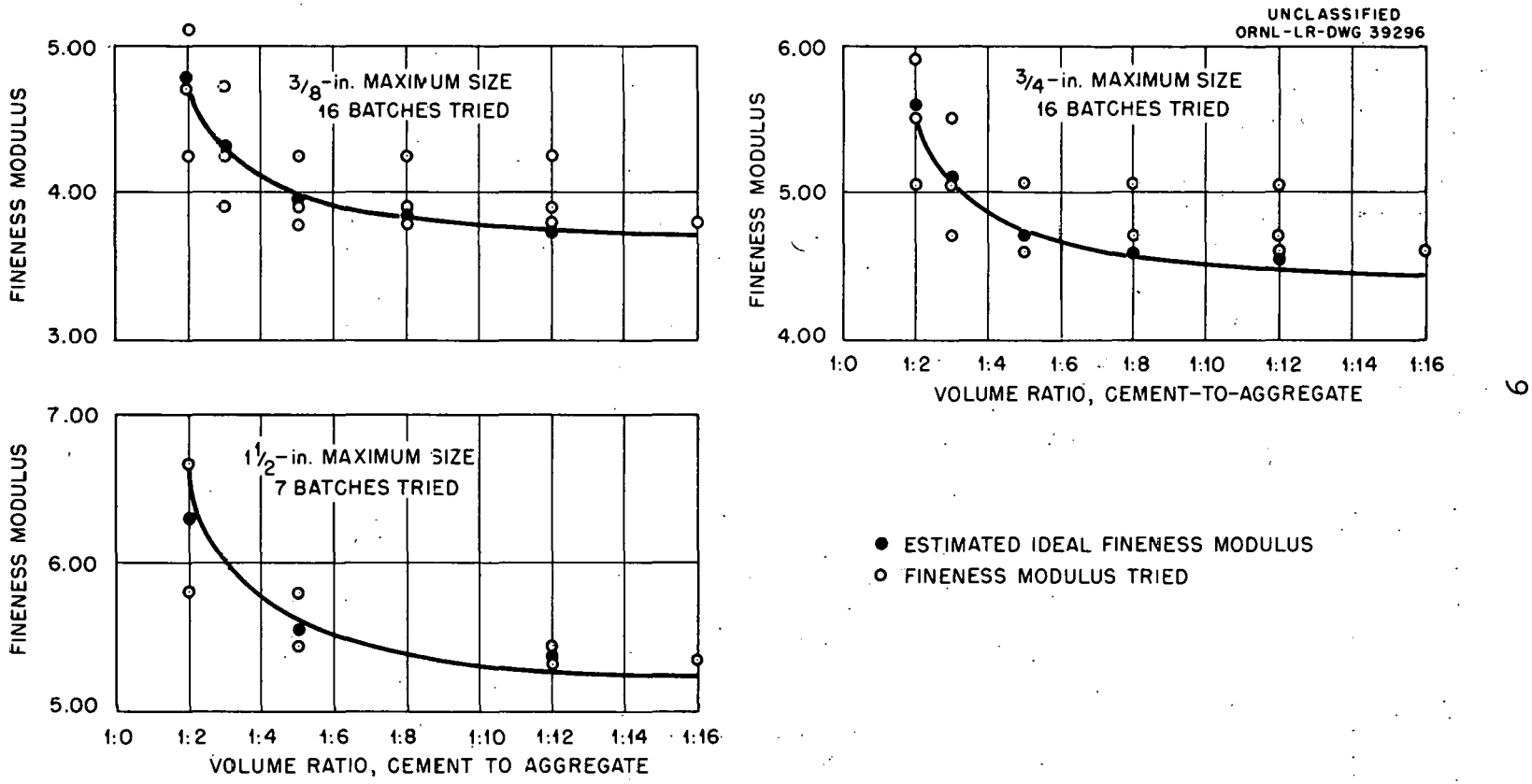

Fig. 4. Ideal Fineness Modulus vs. Cement-to-Aggregate Ratio.

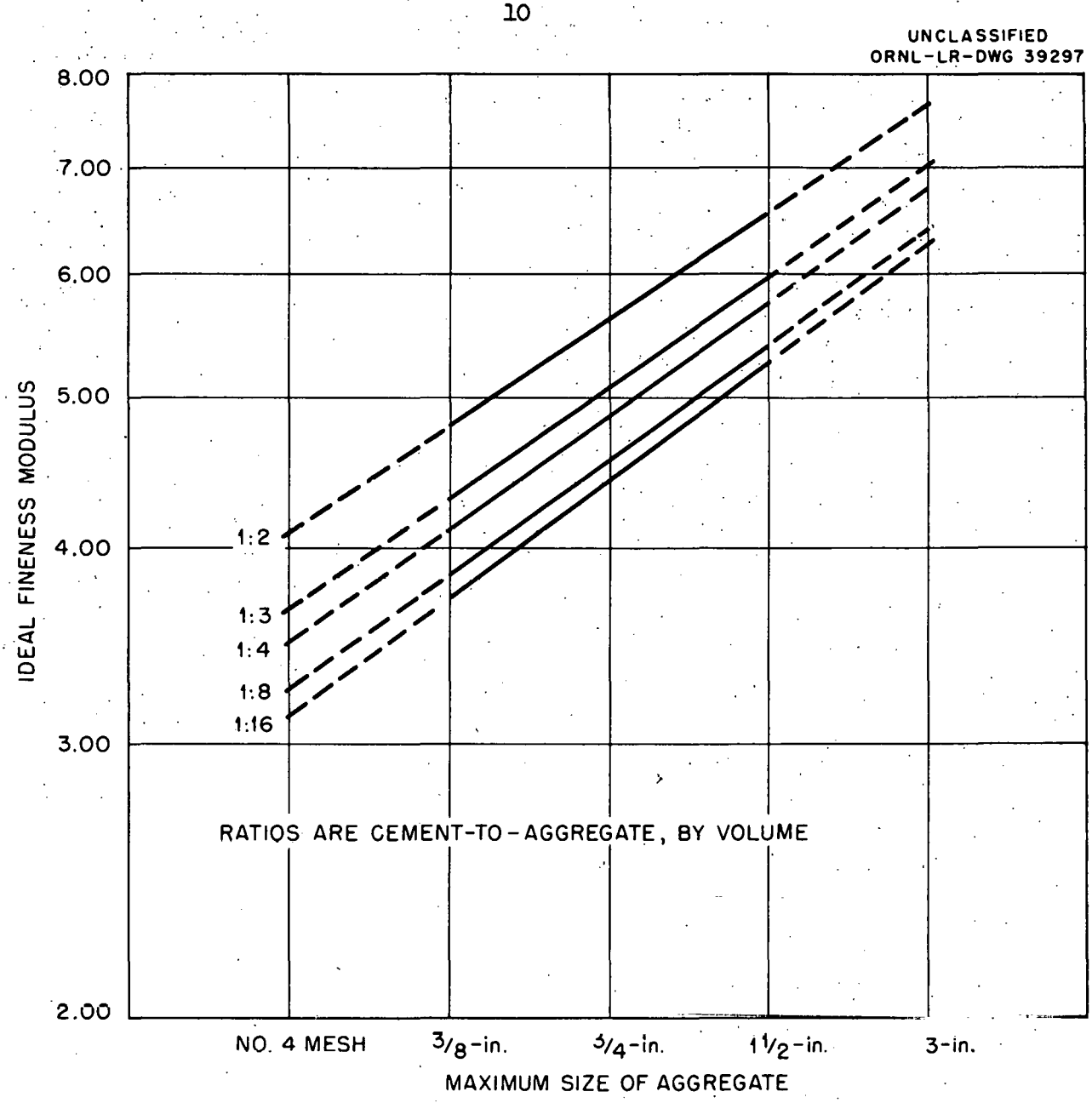

Fig. 5. Ideal Fineness Modulus vs. Maximum Size of Aggregate.

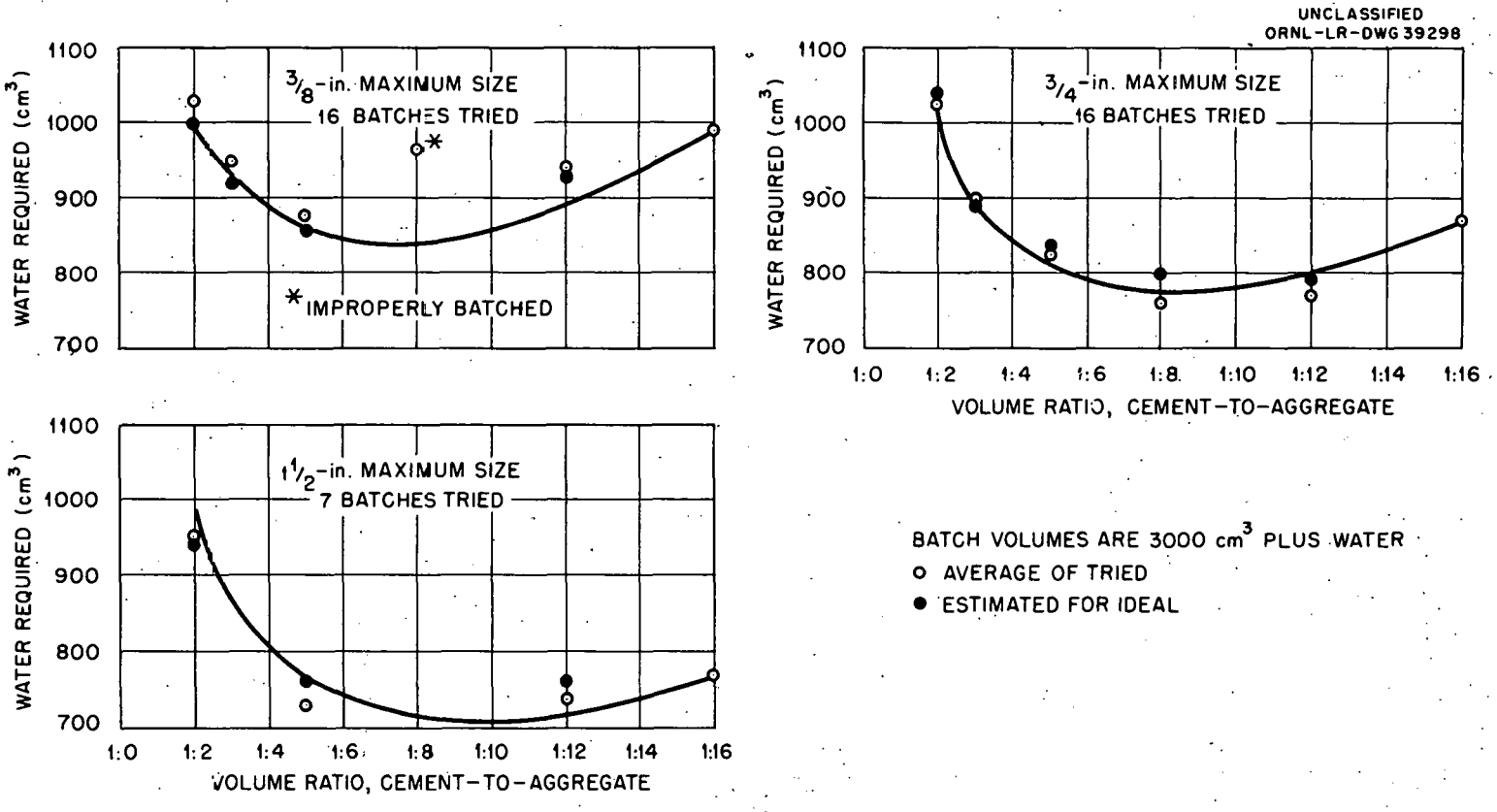

Fig. 6. Water Requirement vs. Cement-to-Aggregate Ratio.

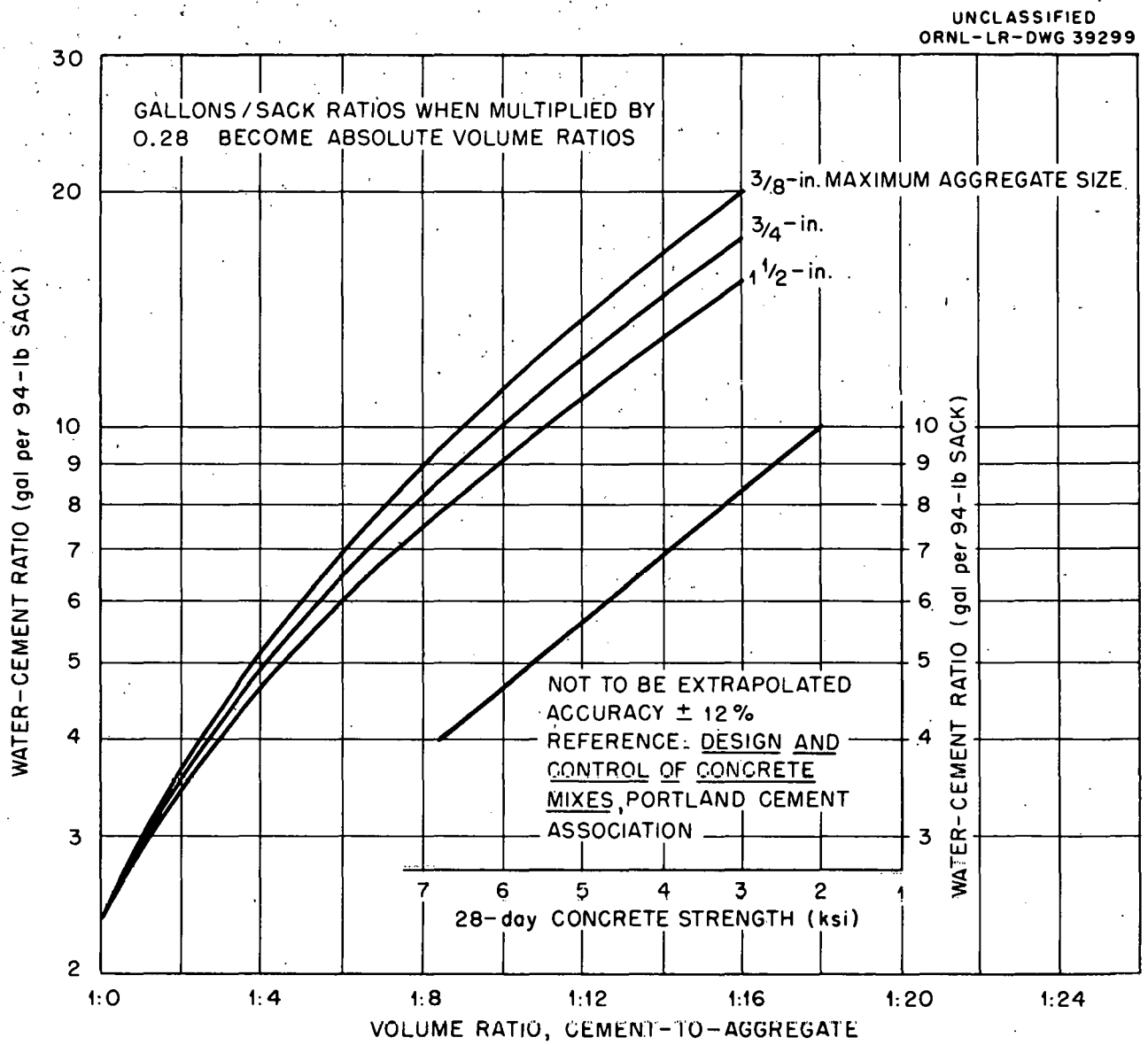

Fig. 7. Water-Cement Ratio vs. Cement-to-Aggregate Ratio.

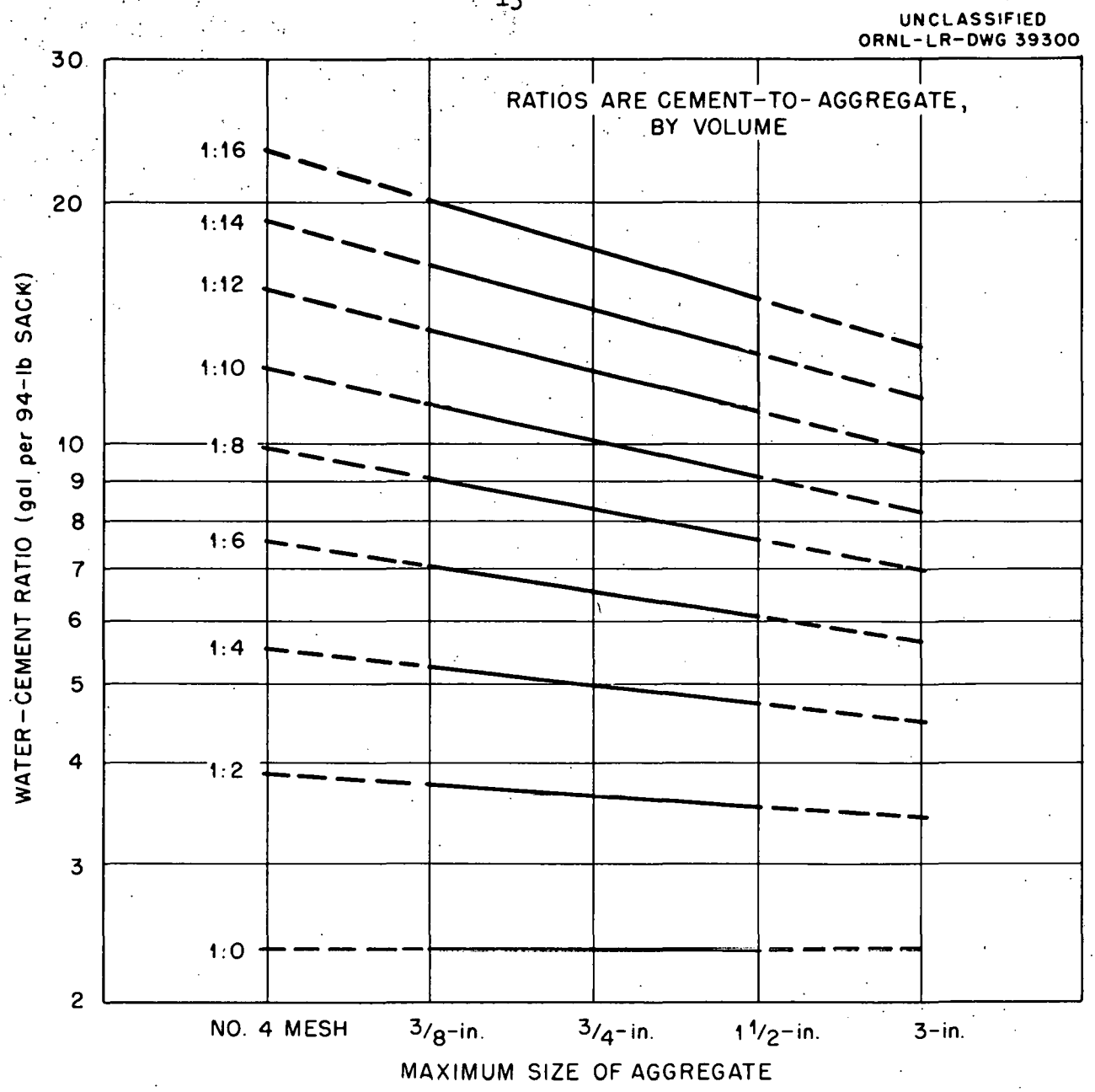

Fig. 8. Water-Cement Ratio vs. Maximum Size of Aggregate.

curves shown in Figs. 6, 7, and 8 represent what seems to be satisfactory agreement regarding the interplay of the three types of plots.

Application of Results

If air voids, usually 1 to 3 per cent of the total volume, are neglected, the following idealized formula results:

Cement Volume + Water Volume + Aggregate Volume = Total Volume of Concrete.

This formula can be written symbolically as:

$$C + W + A = V_t.$$

Cement-to-aggregate ratios (C/A) are unitless volume ratios; the water-cement ratios given in Fig. 7 in gallons of water per 94-lb sack of cement when multiplied by 0.28 also become unitless volume ratios (W/C). Expressing the above total volume formula in terms of these ratios gives

$$C + (W/C)C + (A/C)C = V_t.$$

For selected values of (W/C), (C/A), and V_t, this formula can be solved for the component volumes of cement, water, and aggregate. When V_t is set equal to unity, the component volumes may be expressed as cubic centimeters of material per cubic centimeter of concrete, the coefficients by which component specific gravities may be multiplied to obtain the average specific gravity of the concrete. For example, the average specific gravity of a concrete may be determined as follows:

$$\overline{G} = CG_c + WG_w + AG_a,$$

where G is the specific gravity and the subscripts "c, w, and a" represent cement, water, and aggregate, respectively. The simplicity in use of the

total volume formula lies in the fact that there is a definite relationship between the cement-to-aggregate ratio and the water-cement ratio, as is shown by Fig. 7. Where the coarse and fine aggregate can be proportioned to obtain the desired fineness modulus, component volumes can be computed from the water-cement ratio that corresponds to a desired strength and the cement-to-aggregate ratio consistent with that water-cement ratio. In order to compute the average specific gravity of the concrete, it is only necessary to know, in addition, the specific gravity of the aggregate. (Normally, 3.15 is used for the specific gravity of the cement and 1.00 is sufficiently accurate for the specific gravity of water.) Where the coarse aggregate and the fine aggregate have different specific gravities, an average will be adequate.

Some component volumes per cubic centimeter of concrete, developed from the values indicated by Fig. 8, are shown in Table 2. It should be noted that the values for 3 in. maximum size and No. 4 maximum size are extrapolated values. Multiplying the component volumes of Table 2 by 27 gives volumes in cubic feet of material per cubic yard of concrete; these can be readily converted to batch weights.

To illustrate the effect on concrete density of cement-to-aggregate ratio, Fig. 9 shows a plot for the case of an aggregate having a specific gravity of 4.13 and a 3/4-in. maximum size. Although this plot is developed from the coefficients of Table 2, experimental points are also shown for comparison.

Figure 10 demonstrates the effect of maximum size of aggregate on concrete density. The plot is for an aggregate having a specific gravity of 4.13 and a constant water-cement ratio of 8 gallons per sack, resulting in a concrete strength of approximately 3200 psi. It is important to note that cement-to-aggregate ratios for this plot ranged from 1:6.4 for the No.-4-mesh aggregate maximum size to 1:9.6 for the 3-in. maximum size. This is, of course, the primary reason for the increases in density obtainable with the larger maximum sizes. This plot is also developed from the coefficients of Table 2.

Table 2. Component Volumes per cm^3 of Barytes Concrete
(Not Corrected for 1 to 3 per cent Air Voids)

Material	Cement-to-Aggregate Volume Ratio							
	1:2	1:4	1:6	1:8	1:10	1:12	1:14	1:16
Maximum Aggregate Size: No. 4								
Water	0.266	0.238	0.232	0.235	0.240	0.252	0.262	0.277
Cement	0.245	0.152	0.110	0.085	0.069	0.058	0.049	0.042
Aggregate	0.489	0.610	0.658	0.680	0.691	0.690	0.689	0.681
Maximum Aggregate Size: 3/8-in.-dia								
Water	0.260	0.229	0.221	0.219	0.223	0.230	0.238	0.248
Cement	0.247	0.154	0.111	0.087	0.071	0.059	0.051	0.044
Aggregate	0.493	0.617	0.668	0.694	0.706	0.711	0.711	0.708
Maximum Aggregate Size: 3/4-in.-dia								
Water	0.254	0.219	0.208	0.206	0.207	0.210	0.217	0.224
Cement	0.249	0.156	0.113	0.088	0.072	0.061	0.052	0.046
Aggregate	0.497	0.625	0.679	0.706	0.721	0.729	0.731	0.730
Maximum Aggregate Size: 1-1/2-in.-dia								
Water	0.248	0.210	0.197	0.192	0.191	0.192	0.198	0.203
Cement	0.251	0.158	0.115	0.090	0.074	0.062	0.054	0.047
Aggregate	0.501	0.632	0.688	0.718	0.735	0.746	0.748	0.750
Maximum Aggregate Size: 3-in.-dia								
Water	0.243	0.201	0.185	0.178	0.174	0.175	0.177	0.179
Cement	0.252	0.160	0.117	0.091	0.075	0.063	0.055	0.048
Aggregate	0.505	0.639	0.698	0.731	0.751	0.762	0.768	0.773

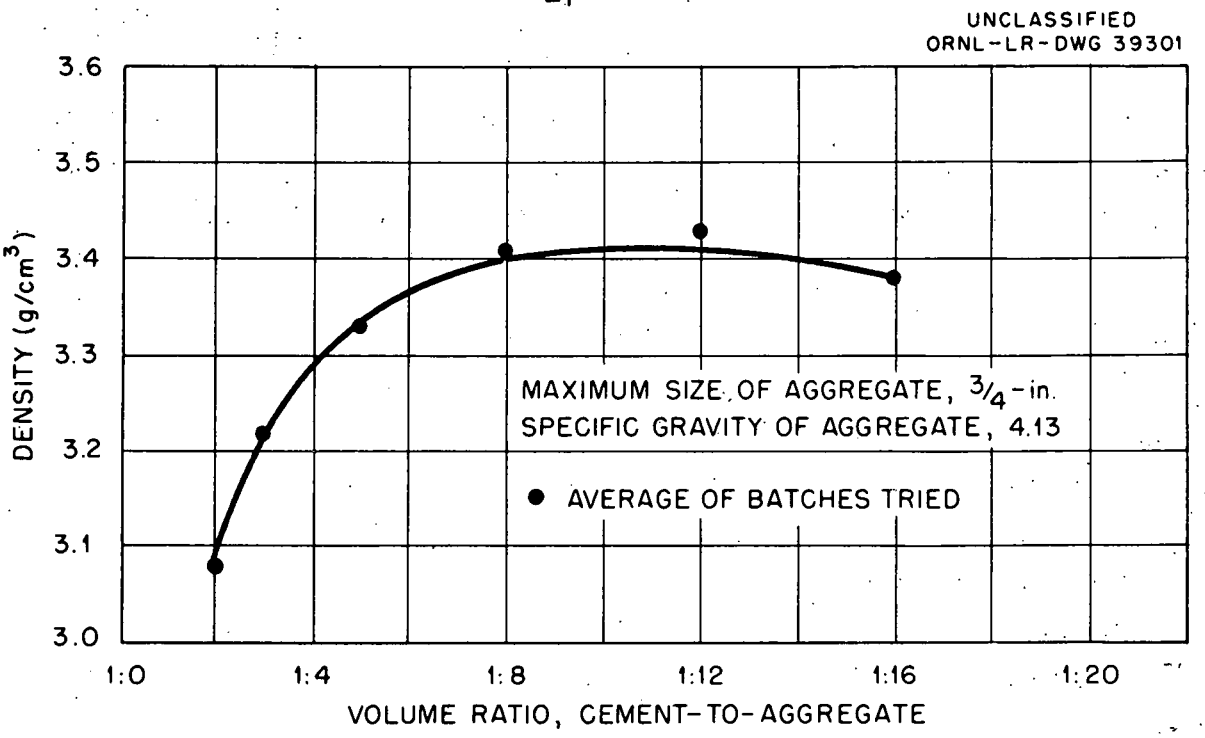

Fig. 9. Density vs. Cement-to-Aggregate Ratio.

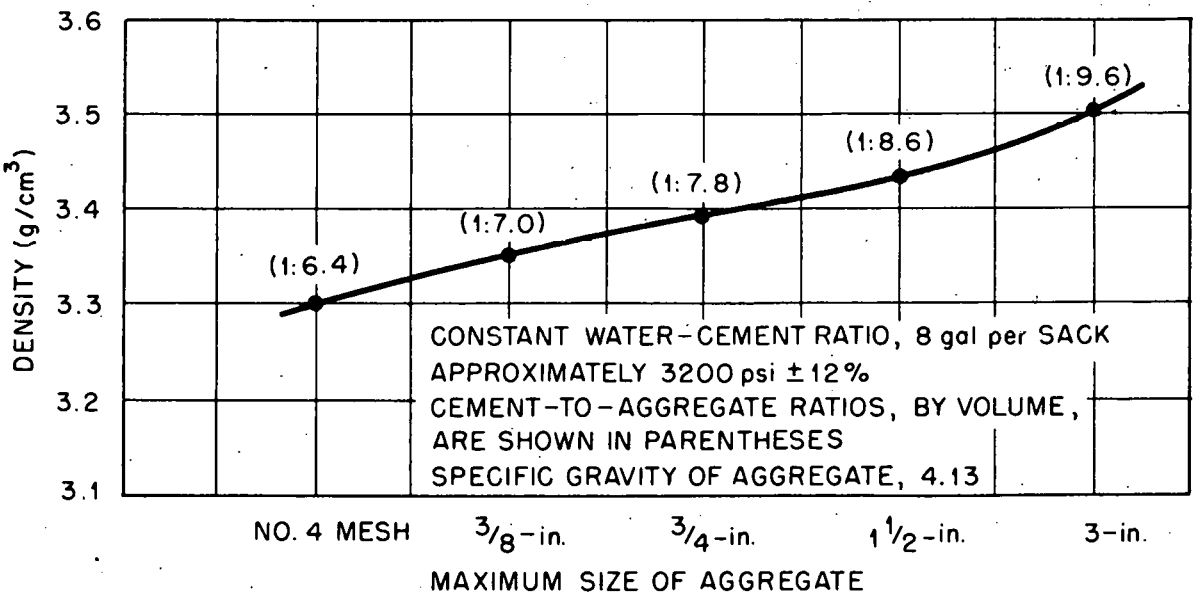

Fig. 10. Density vs. Maximum Size of Aggregate.

A plot showing concrete density as a function of the specific gravity of the aggregate has not been given, since for a given cement-to-aggregate ratio and a specific maximum size of aggregate, the relationship is obviously linear.

Conclusion

These data are offered largely as aids for the evaluation of the potential effectiveness of a concrete shield, and should not be considered as strict rules by which all concrete must abide. In their conception, they are idealized or mean values, and only when all variables are properly controlled will the field results approach these idealized laboratory results. However, by interpolations from Table 2 or by plots similar to Figs. 9 and 10, probable maximum concrete densities may be estimated. Even in situations approaching ideal, the laboratory results are unequivocably applicable only when the aggregates under consideration are barytes. However, the data should be applicable to other aggregates if the following points are remembered:

a. Crushed aggregates like barytes are more angular and require more cement paste than naturally rounded aggregates;

b. Relatively soft aggregates like barytes are usually covered with dust particles and will normally require more mixing water than harder, tougher aggregates;

c. Barytes aggregates do not require the extra cement paste to fill cellular voids that some of the vesicular artificial aggregates require.

Densities predicted by these data are, of course, contingent on the use of the recommended gradations. The desired gradation can usually be obtained, however, by the proper proportioning of fine and coarse aggregates. The following formula is useful for this task:[2]

$$P_f = \frac{M_c - M_m}{M_c - M_f} (100),$$

where

P_f = percentage of fine aggregate in a mixture of coarse and fine aggregates,

M_m = desired fineness modulus of the mixture,

M_c = fineness modulus of the coarse aggregate in the mixture,

M_f = fineness modulus of the fine aggregate in the mixture.

Fineness moduli greater than these may cause the fresh concrete to be too harsh and should not be used. Fineness moduli less than those recommended are acceptable, but for best results they should be held to within 5 per cent of the recommended moduli.

The water contents recommended should give slumps of 0 to 1 in. An increase of 10 per cent in the water content should increase the slump by 3 to 5 in.

II. RADIATION ATTENUATION CHARACTERISTICS OF BARYTES CONCRETE COMPONENTS

Introduction

The relative importances, with respect to radiation shielding efficiency, of the components in a shielding concrete are worthy of special attention in the proportioning of a mix. Density, while it is of primary importance with regard to gamma-ray shielding, cannot be adopted as the sole criterion. Neutron attenuation is more dependent upon the presence of light nuclei, and in some instances it may be desirable to compromise density in order to gain a more efficient neutron shield. While the previous discussion deals principally with the density of concrete, and hence gamma-ray attenuation, this section is chiefly concerned with the attenuation of neutrons by concrete. During the experiments supporting this portion, gamma-ray dose measurements were made, but no detailed analysis of the gamma-ray data has been attempted. Although this study gave particular attention to barytes concrete, the data should nevertheless provide information useful in the evaluation of other shielding concretes.

In the following discussion, neutrons are classified by particular energy groups. Those neutrons having energies of approximately 0.025 ev are classified as thermal-energy neutrons. All neutrons of energy greater than 0.2 Mev, the threshold energy of the fast-neutron dosimeters used, are classified as fast neutrons. Neutrons with energy above 0.025 ev but less than 0.2 Mev, are grouped as epithermal neutrons. It is convenient to make one subclassification: fast neutrons of energy less than 2 Mev may alternately be termed intermediate-energy neutrons.

In penetrating a material fast neutrons may undergo various interactions with the nuclei of the material. From a shielding viewpoint, the most important of these interactions are inelastic scattering and elastic scattering.

In inelastic scattering the incident or "projectile" neutron enters a target nucleus to form a compound nucleus. It is then re-emitted with appreciably lowered energy, and is usually quickly slowed to thermal energy and absorbed. Thus inelastic scattering is usually considered an absorption process. In elastic scattering, however, an incident neutron colliding with a shield nucleus changes direction and suffers some loss of energy. Since energy decrements from collisions with heavy nuclei are small, elastically scattered neutrons may diffuse through the material with only slight degradation in energy. On the other hand, a neutron undergoing an elastic scattering with hydrogen may lose a large part or all of its original energy.

The probability, per centimeter, that a neutron will undergo a specific interaction is represented by the macroscopic cross section, Σ, of the target material for that particular interaction. Since for shielding purposes the quantity of interest is the effective removal of the incident neutron, a special cross section, the macroscopic removal cross section, Σ_R, is used. The removal cross section is simply the total cross section for inelastic scattering, plus some fraction of the elastic scattering cross section. Since, in general, elastic scattering cross sections are very small for high-energy

neutrons, fast-neutron removal cross sections are essentially determined by the inelastic scattering process. The elastic cross section of hydrogen is high below 1 Mev, but diminishes rapidly above 1 Mev. Thus, in the fast-neutron energy range, many other materials are as effective as or more effective than hydrogen as a neutron shield.

With the removal or degradation of fast neutrons, a spectrum predominant in epithermal and thermal neutrons remains. In order for the shield to be effective, these neutrons must also be removed. Since the capture cross section varies inversely with the square root of the neutron energy, sufficient hydrogen or other moderating material to slow the epithermal neutrons to energies where they can easily be captured must be included in the shield.

Because effective removal cross sections are generally lower for fast neutrons than for slower ones, the attenuation of a fission spectrum of neutrons by a thick shield can usually be characterized by the effective removal cross section for an energy of approximately 8 Mev. It should be cautioned that the fast-neutron removal concept does not apply unless neutrons of lower energies are being attenuated at least as efficiently as the very fast neutrons. With concretes of normal water content this criterion is adequately satisfied;[8,9] however, some uncertainty exists regarding the attenuation efficiency of drier concretes.

Description of Experimental Geometry and Materials

In this study, aluminum cans (see Fig. 11) filled with the component materials of barytes concrete were placed near a fission source and the emergent radiation doses behind various shield assemblies were studied. These studies were performed at the Lid Tank Shielding Facility (LTSF), so-called because of its geometric relationship to the ORNL Graphite Reactor (see

8. A. F. Avery and J. E. W. Simmons, The Effect of Hydrogen Content on Neutron Dose Attenuation in Portland Concrete (British Report, 1959), AERE R/R-2782.
9. E. P. Blizard and J. M. Miller, Radiation Attenuation Characteristics of Structural Concrete (Oak Ridge National Laboratory, 1958), ORNL-2195.

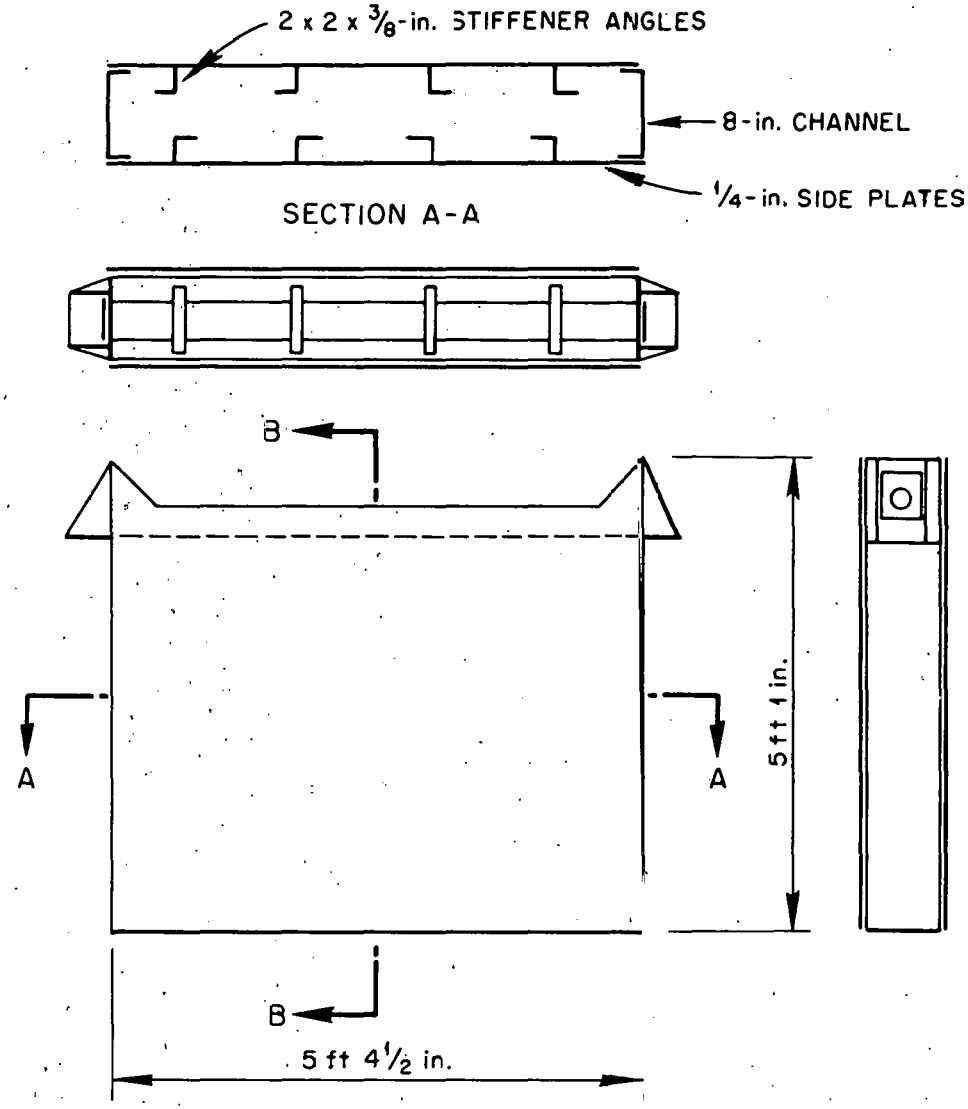

SIDE PLATES ARE 1100-f ALUMINUM. ALL OTHER PARTS ARE STRUCTURAL (6061-T6) ALUMINUM.

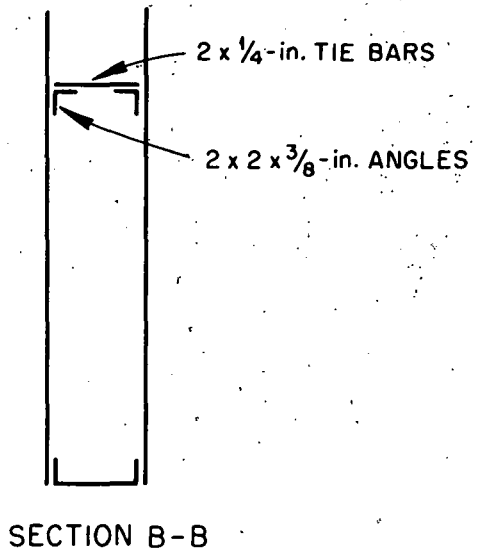

Fig. 11. Aluminum Cans to Contain Shield Materials.

Fig. 12). A horizontal core hole through the reactor shield acts as a leakage duct for thermal neutrons from the reactor core. The U^{235} in a U^{235}-enriched uranium plate located across the opening at the outer face of the shield is caused to fission by the escaping thermal neutrons. The uranium plate, since it serves as a source of fission neutrons and gamma rays, is called the source plate. The lid tank proper is a large steel tank located immediately behind the reactor shield; it carries the source plate assembly in one wall. A smaller configuration tank is inside the lid tank. The water in the lid tank helps to prevent radiation leakage into areas where it is not desired. An inflated air bag fills the gap between the configuration tank and the source plate, thus preventing the water medium from entering this region and allowing the fission radiation to pass through essentially unaffected.

Radiation intensities were measured by instruments placed in water-filled aluminum auxiliary tanks located immediately behind the test cans. The technique of using auxiliary tanks instead of a water-filled configuration tank avoids the possibility of water collecting between the test cans; however, the 1/8-in.-thick walls of the aluminum auxiliary tank have to be considered in data analysis.

In the data analysis, attenuation characteristics of test shields were compared with the attenuation characteristics of a water shield. Radiation intensities behind a water shield were obtained by filling the configuration tank with water and measuring the intensities in the tank at various points along the Z axis, the perpendicular, horizontal centerline of the source plate.

The shielding materials studied were barytes aggregate, barytes aggregate mixed with cement in normal proportions, and barytes concrete. Both the coarse aggregate and fine aggregate used were crushed barytes. Relatively speaking, it can be said that the fine aggregate was rather coarse and the coarse aggregate rather fine. The coarse aggregate used was a 1-in. maximum-size

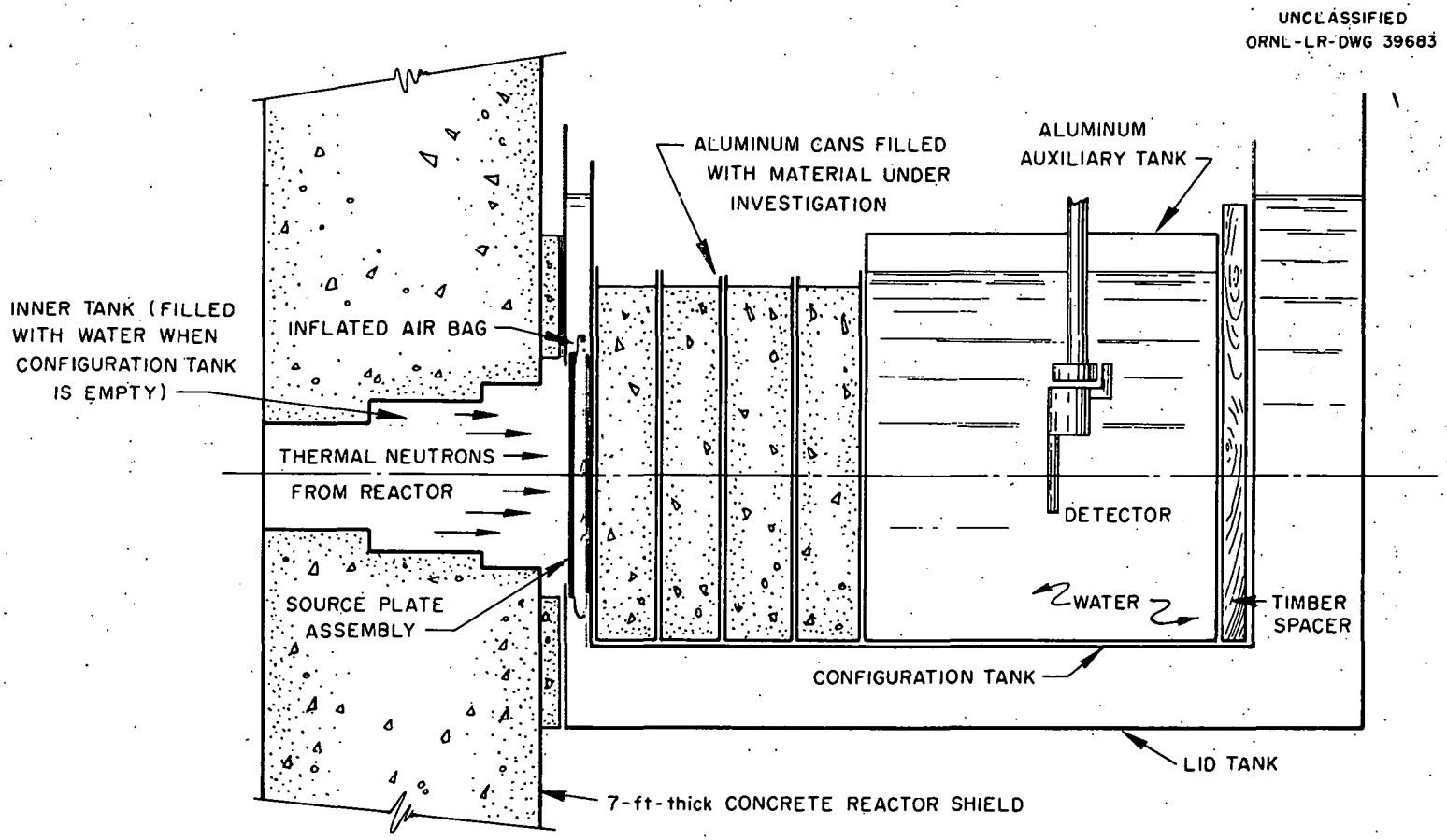

Fig. 12. Schematic Drawing of Lid Tank Geometry.

aggregate with a fineness modulus of approximately 6.06; its worst feature, however, lay in the fact that approximately 30 per cent of it was smaller than the No. 4 sieve size and 4 per cent of it smaller than the No. 100 sieve size. The fine aggregate, on the other hand, had the rather high fineness modulus of 3.2, with all material passing through the No. 4 sieve. Because the aggregates used for the first series of test (barytes aggregate, alone) were intended to also serve for the two subsequent series, the coarse and fine aggregates were proportioned for the final objective. On the basis of a 1:8 cement-to-aggregate ratio, it was determined (from Fig. 5) that a combined fineness modulus of approximately 4.95 should be sufficient. For convenience, the aggregate proportions were rounded off to two parts fine to three parts coarse.

Barium sulphate, the primary compound in barytes, has a specific gravity of 4.5, but barytes usually has a specific gravity somewhat lower; from 4.0 to 4.4 is normal. The barytes aggregate used[10] had the rather low saturated-surface-dry specific gravity of 4.04, but was considered sufficiently dense for this study. The aggregate had a moisture-absorption coefficient of 3.7 per cent by weight and a moisture content of 1.7 per cent by weight.

The limiting criterion for the selection of the 1:8 cement-to-aggregate ratio was strength rather than density. It was decided that the concrete should have an average strength of at least 3000 psi in order to be comparable to concrete normally used in construction. A water-cement ratio of approximately 8 gallons per sack of cement should result in concrete with a strength of approximately 3200 psi. Figure 7 indicates that for an aggregate of 1-in. maximum size and a water-cement ratio of 8 gallons per sack, a 1:8 cement-to-aggregate ratio should develop the desired strength. Although it was recognized beforehand that the abrasion from repeated mixings (three

---

10. These aggregates were mined at Sweetwater, Tennessee. Those used in the first portion of the study were mined at Cartersville, Georgia.

times) would cause the aggregate gradation to become finer and that there would be losses due to handling, the experiment proceeded on the above theoretical basis.

In the first series of tests, six aluminum cans were filled with 15,110 lb of barytes aggregate which had been blended by a conventional 5-yd concrete-mixing truck. Under mild vibration, the aggregate settled to an average unit weight of 168 lb/cu ft, or an average density of 2.69 g/cc. Radiation measurements were then made behind two, four, and six cans, in that order.

The cans were then emptied and the contents returned to the truck mixer. Sixteen sacks (1500 lb) of Type-I Portland cement were then added, and the mixture was blended. Truck weights empty and loaded indicated that approximately 200 lb of material was unaccounted for, but the loss was so small that the difference was assumed to have no effect on the cement-to-aggregate ratio. The barytes-cement mixture was vibrated lightly and an average unit weight of 167 lb/cu ft was obtained - average density, 2.67 g/cc. The filled cans were then returned to the configuration tank one at a time and radiation intensities measured behind each added increment of shield.

As in the case previously described, the cement and aggregate were returned to the mixing truck after the second series of tests had been completed. As there was no way of estimating the effect on the mix of material losses, the water was added cautiously. When 1,230 lb of water had been added the fresh concrete appeared to be workable enough to be emptied (measured slump, 2 in.). It might be noted that the mixing truck, even with a contained volume of less than 4 cu yd, had difficulty mixing and expelling the high-density concrete. In fact, a large amount of concrete was not recoverable from the truck with the consistency desired and as a consequence only five cans were filled for the final series of tests.

As the concrete was being placed in the cans, five compression test cylinders, 6-in.-dia by 12 in., were taken. Six smaller cylinders, 3-in.-dia

by 6 in., were also taken to have a check on the unit weights determined by the total-weight versus total-volume method.

In the process of returning the barytes-cement mixture to the mixing truck, an additional 570 lb of material was lost. Calculations reveal, however, that the cement-to-aggregate ratio remained essentially constant. The average density of the concrete as determined from the small 3-in.-dia cylinders was 3.27 g/cc, the same value as the total weight in the cans divided by the total volume. The procedure described in Section I for estimating concrete densities predicts an uncorrected concrete density of 3.35 g/cc for a 1-in. maximum size aggregate, a 1:8 cement-to-aggregate ratio, and an 8-gallon-per-sack water-cement ratio. When this value is corrected for the air voids normally occurring in concrete, approximately 2 per cent, the result is 3.28 g/cc, which is in close agreement with the experimental value. On the basis of the weight relationships established above, the calculated water content before hydration was 8.92 per cent by weight. The amount of hydrated water after a 28-day curing period was approximated[1] as 13 per cent by weight of the cement. The final density was determined to be 3.30 g/cc with a water content of 9.91 per cent by weight.

The concrete in the aluminum cans was cured by maintaining approximately 1 in. of water above the level of the concrete. The cylinders were left in the molding containers during the entire 28-day curing period to simulate the same curing conditions to which the shield was subjected. Moist conditions here were maintained with wet burlap.

The 6-in.-dia cylinders were compression tested at the end of the curing period according to standard ASTM procedures. The five cylinders tested had an average strength of 3200 psi, with a ± 6 per cent maximum deviation from the average.

Instrumentation

The detection instruments conventionally employed by the Lid Tank Shielding Facility (LTSF) were used for this study. The following remarks with regard to these instruments were made merely to specify the nature of the instrumentation in order to qualify detection results. Detailed descriptions of these instruments have been presented by D. W. Cady.[11]

Four instruments were used to measure the thermal-neutron flux, nv_{th} (neutrons$\cdot$cm$^{-2}\cdot$sec^{-1}). Three of these instruments are parallel-plate fission chambers, differing primarily by the amount of U^{235} contained and hence in their sensitivity. The uranium in two of these chambers is deposited on a nickel plate over a circular area of approximately 3 in. in diameter; in the third chamber, the area is reduced to approximately that of a 1/2-in.-dia circle. The fourth instrument is a B^{10}-enriched BF_3 counter, 12-1/2 in. long.

The thermal-neutron instruments are all normalized to a thermal-neutron flux curve determined with gold foils. These normalization factors are then used for count-to-flux conversions.

Both of the instruments used for fast-neutron dose rate detection are Hurst dosimeters. The Hurst dosimeter is a proton-recoil instrument, its primary feature being a polyethylene-lined chamber filled with ethylene gas. The sensitivity of the Hurst dosimeter is largely controlled by the volume of this chamber. The instrument designated FN-62 has a larger gas chamber and is thus more sensitive than the instrument called FN-82. A pulse-height integrator weights the ionization pulses from the recoil protons and sums the total weighted counts. The Hurst dosimeters were calibrated against the known fast-neutron dose rate at a given distance from a polonium-beryllium source.

---

11. D. W. Cady, The Lid Tank Shielding Facility at Oak Ridge National Laboratory. Part III. Instrumentation (Oak Ridge National Laboratory, 1959), ORNL-2587.

One of the two instruments used for gamma-ray dose-rate detection is a 50-cc, carbon-CO_2 ion chamber. The average ionization current produced in this chamber is directly proportional to the gamma-ray dose rate. The instrument is calibrated against the known gamma-ray dose rate at a standard distance from a radium source. The second of the two gamma-ray dose instruments used is a scintillation counter designated at the LTSF as PM(A). It consists of an anthracene crystal mounted on an RCA-type 5819 energy photomultiplier. The current output of the photomultiplier is measured with an electrometer. The PM(A), like the 50-cc ion chamber, is calibrated against the known gamma-ray dose rate from a radium source.

All dose-rate measurements made are assumed to be accurate to only ±10 per cent.

Test Results

The results of the detection measurements made behind various shield configurations are shown graphically in Figs. 13 through 21. Since these results are given on a per-watt basis, it is important to note that although a source plate power of 5.18 watts was assumed for this study, more recent measurements of this value[12] give 5.22 watts. The difference, however, is well within the limits of experimental error. Where repeated measurements at a point differed by less than 10 per cent, a single, averaged point is shown. Otherwise, all experimental points are shown.

Figures 13, 14, and 15 show thermal-neutron fluxes, nv_{th} (neutrons·cm^{-2}·sec^{-1}), behind various test shields. Frequently, scattering from the rear of the auxiliary tank caused the rear-most readings to be high. Since this is a recognized effect, it is taken into account in the drawing of the curves.

---

12. D. R. Otis, The Lid Tank Shielding Facility at Oak Ridge National Laboratory. Part II. Determination of the Fission Rate of the Source Plate (Oak Ridge National Laboratory, 1959), ORNL-2350.

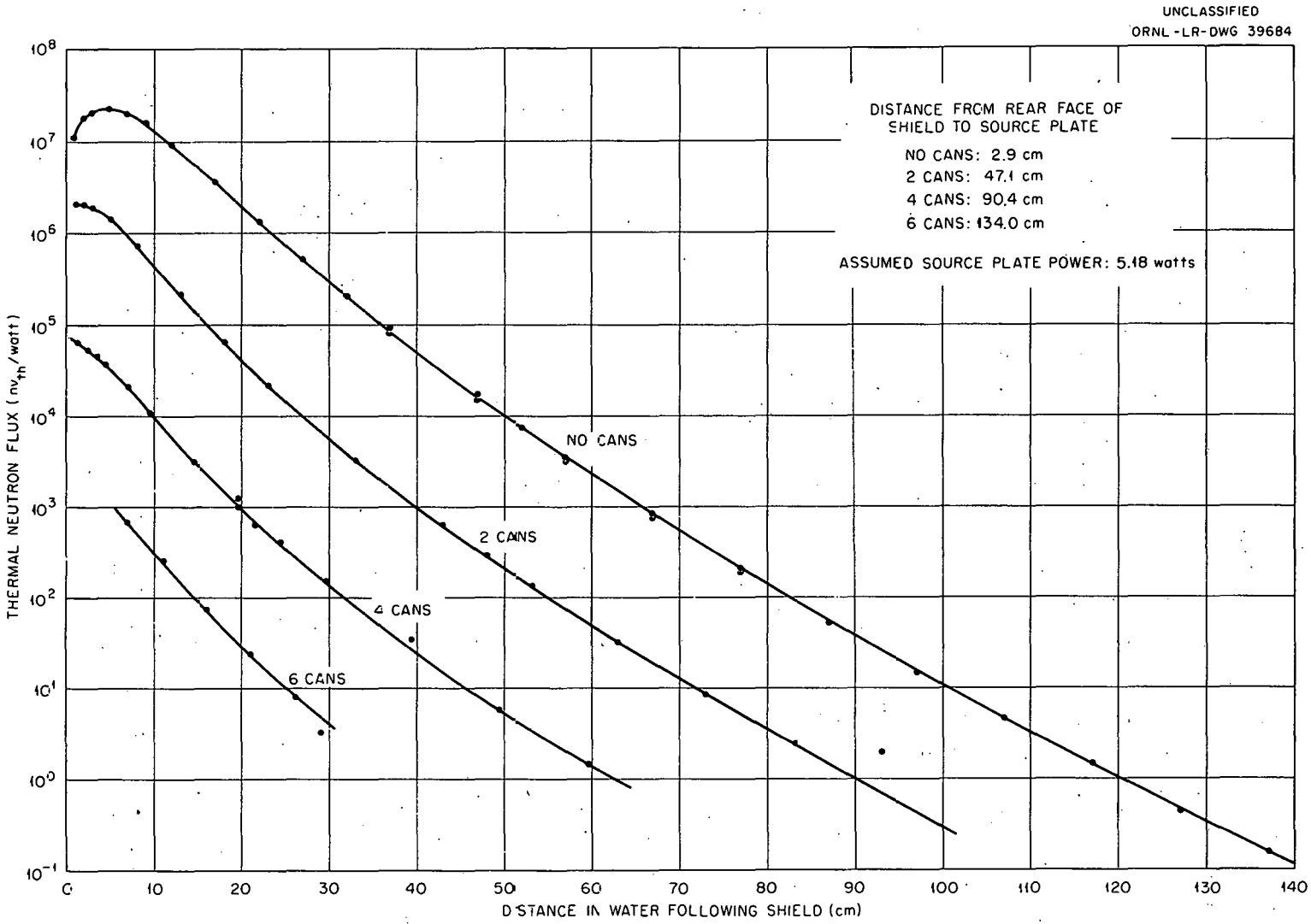

Fig. 13. Thermal Neutron Flux in Water Following Cans of Barytes Aggregate.

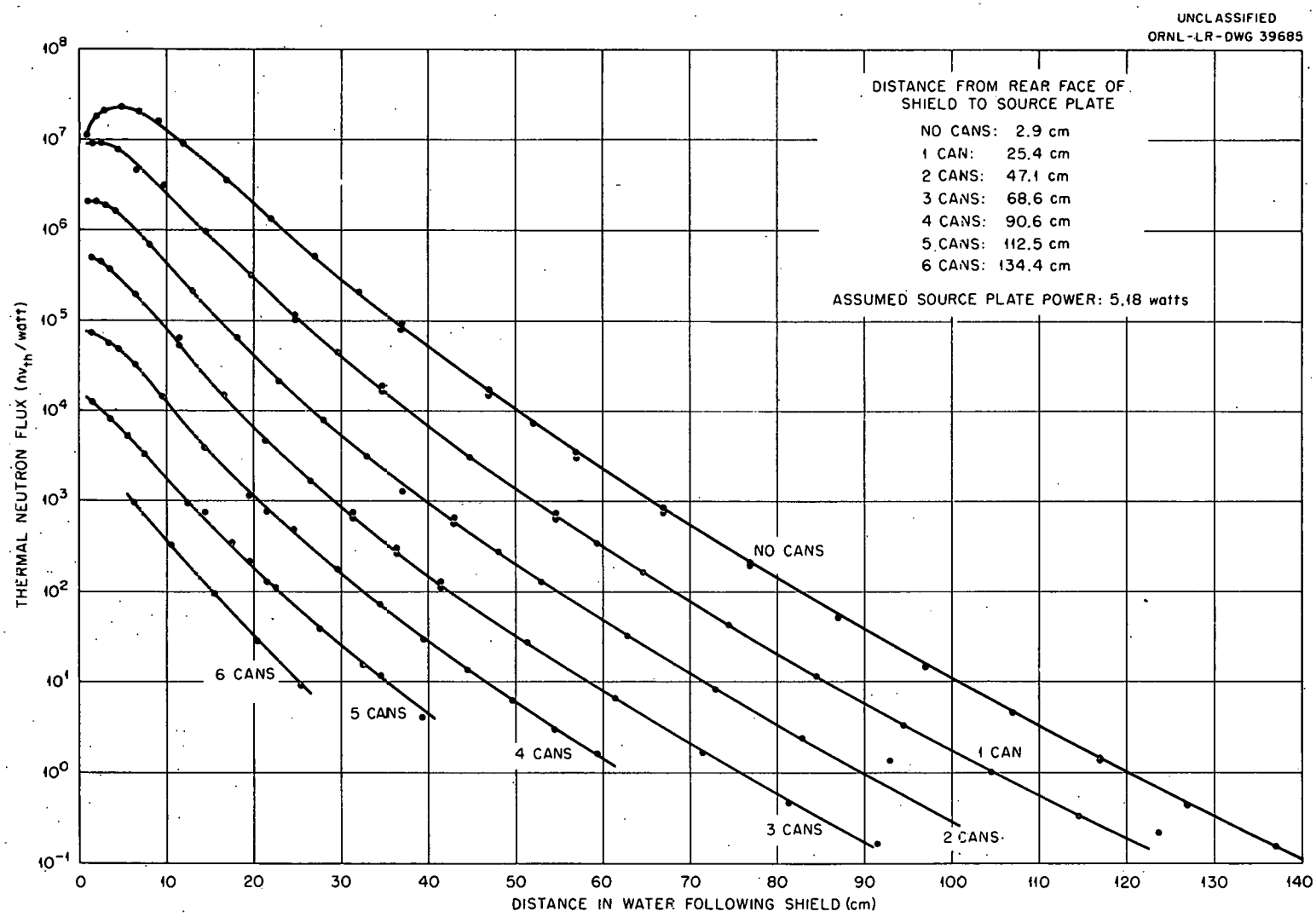

Fig. 14. Thermal Neutron Flux in Water Following Cans of Barytes Aggregate Plus Cement.

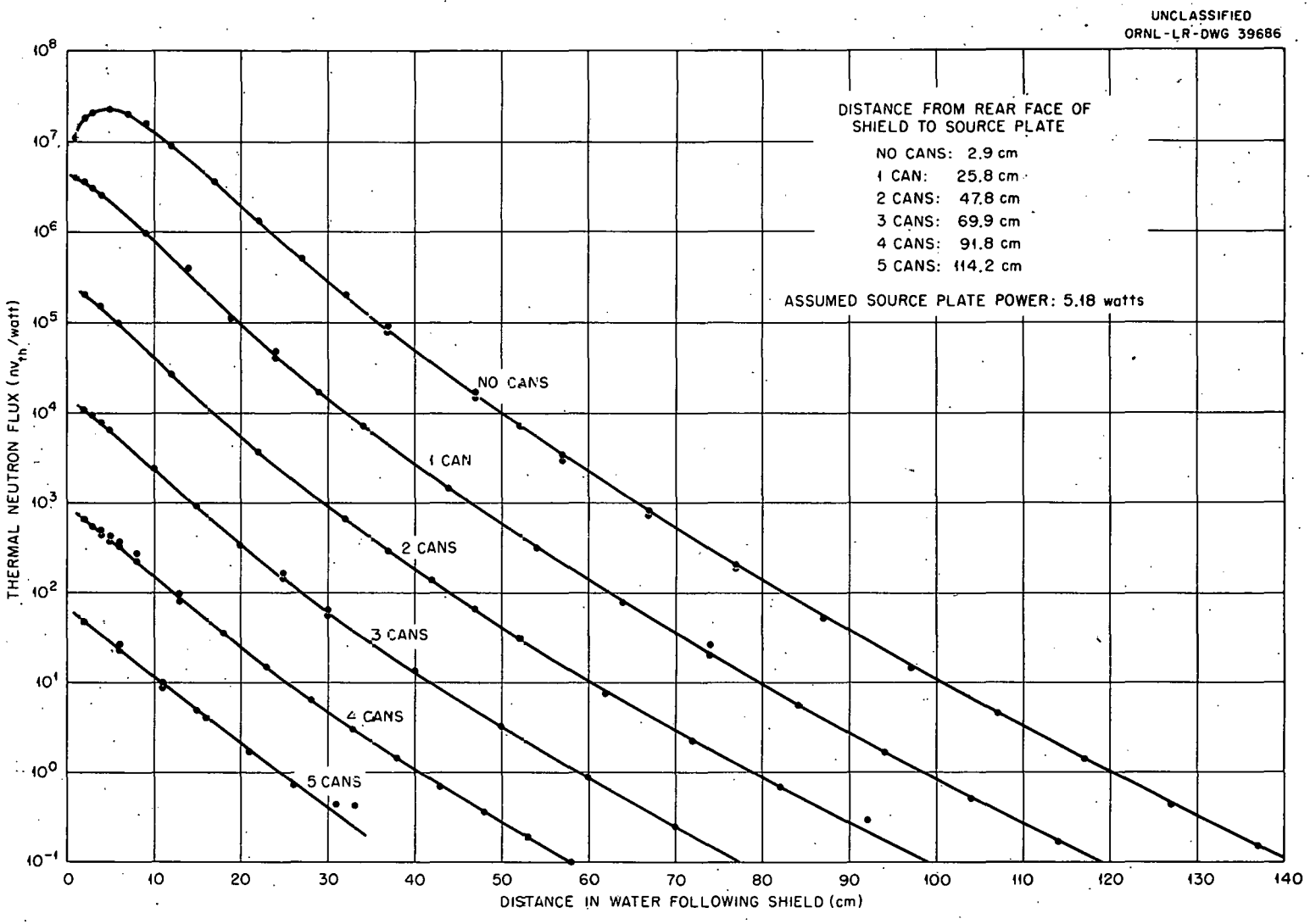

Fig. 15. Thermal Neutron Flux in Water Following Cohs of Barytes Concrete.

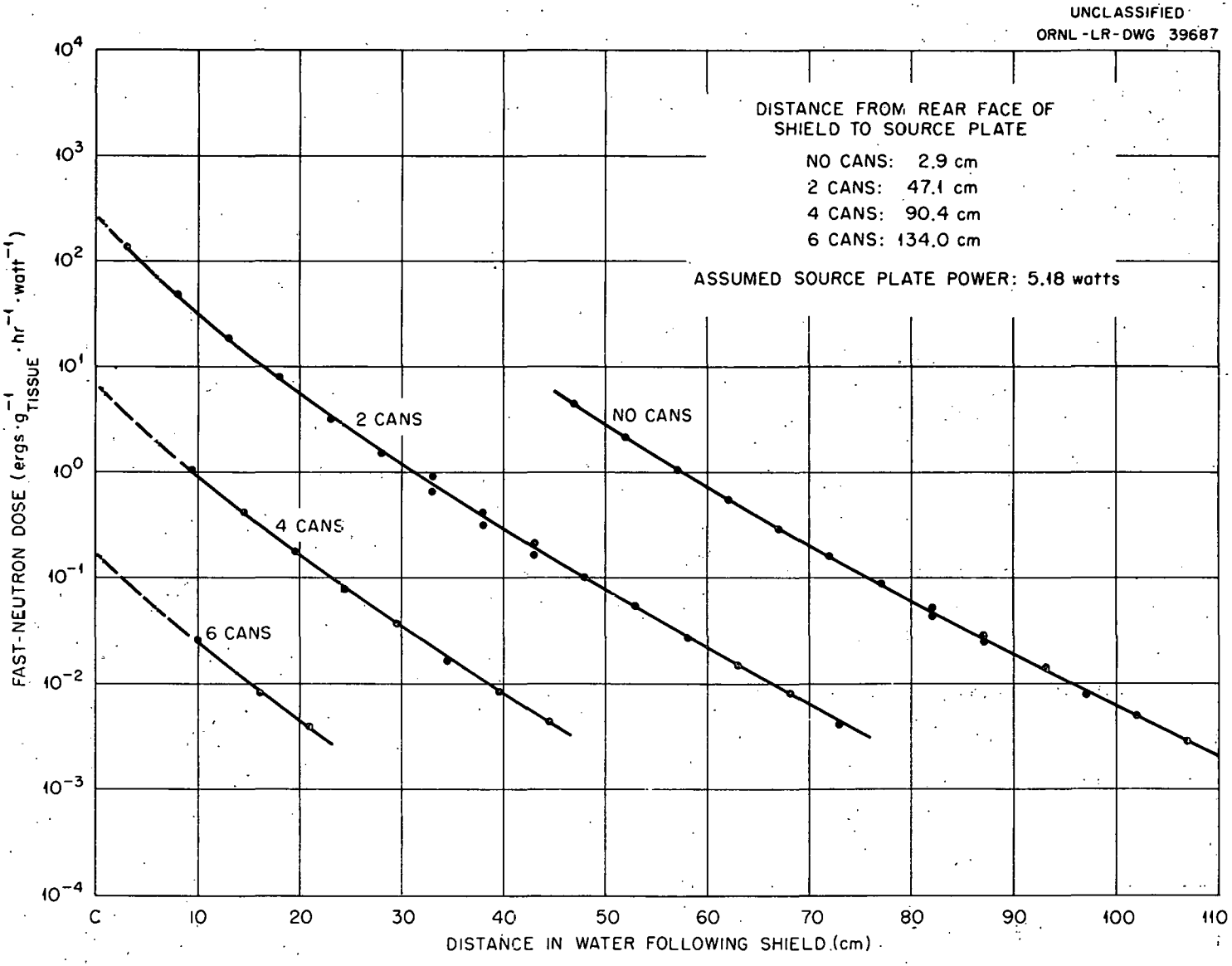

Fig. 16. Fast-Neutron Dose in Water Following Cans of Barytes Aggregate.

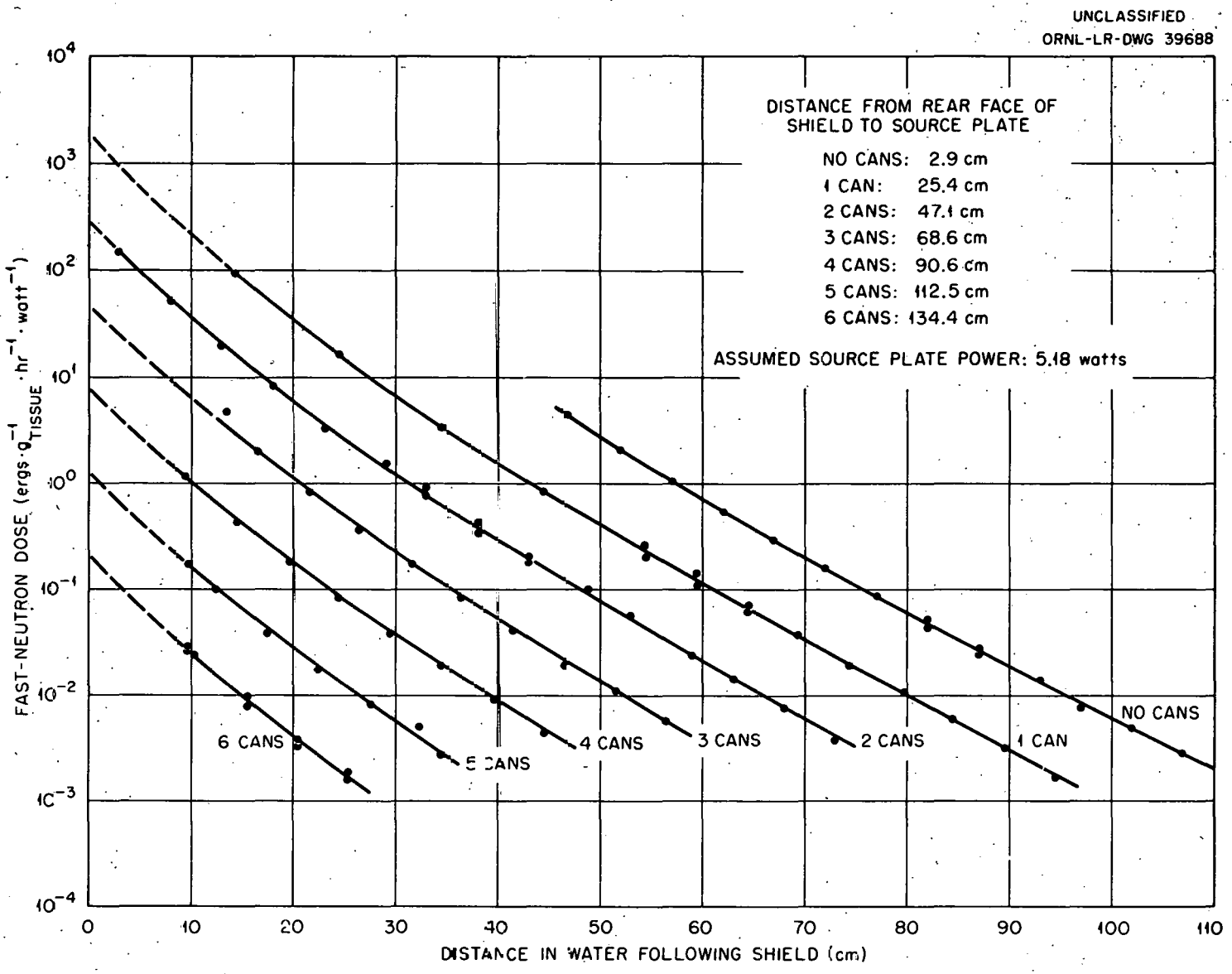

Fig. 17. Fast-Neutron Dose in Water Following Cans of Barytes Aggregate Plus Cement.

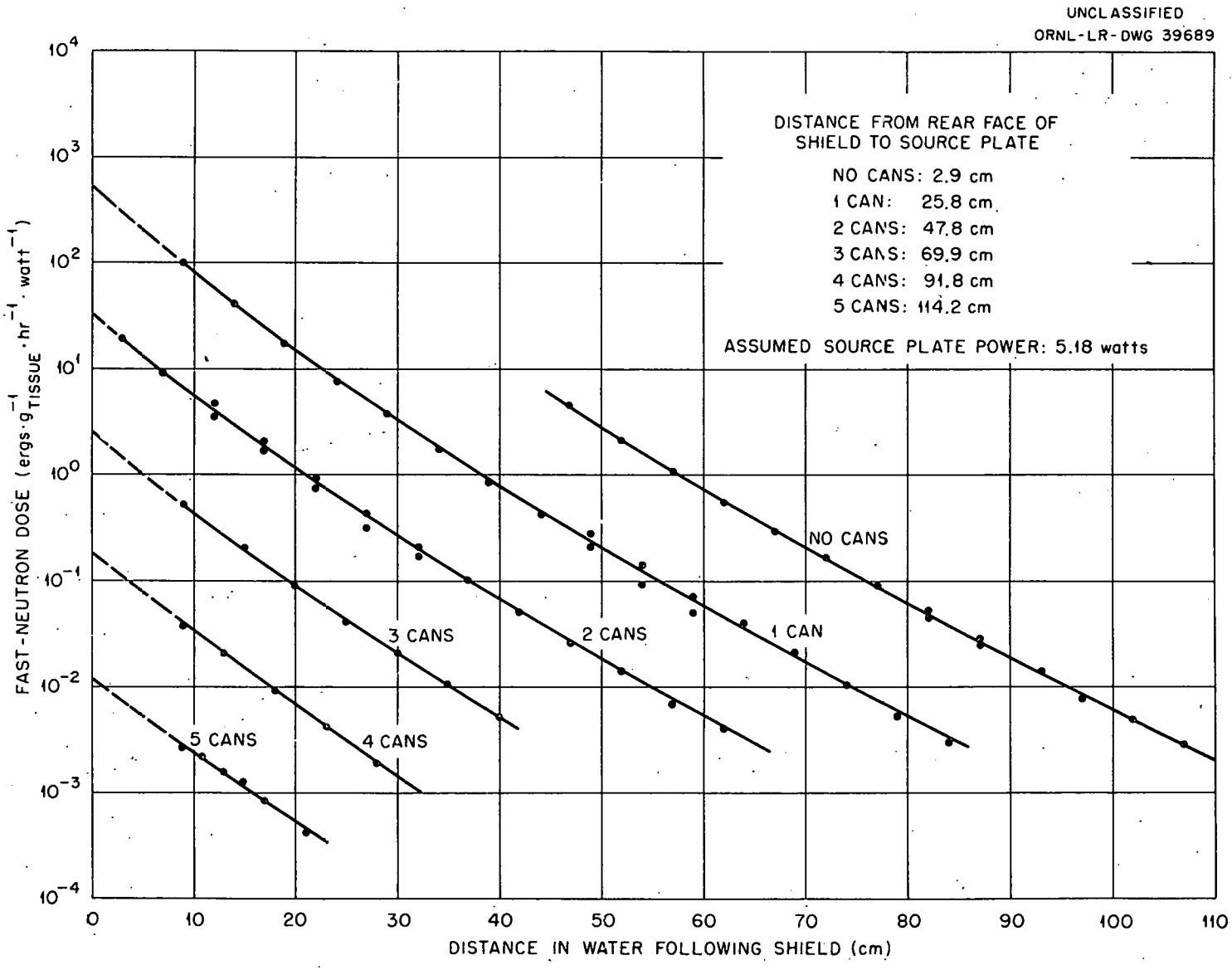

Fig. 18. Fast-Neutron Dose in Water Following Cans of Barytes Concrete.

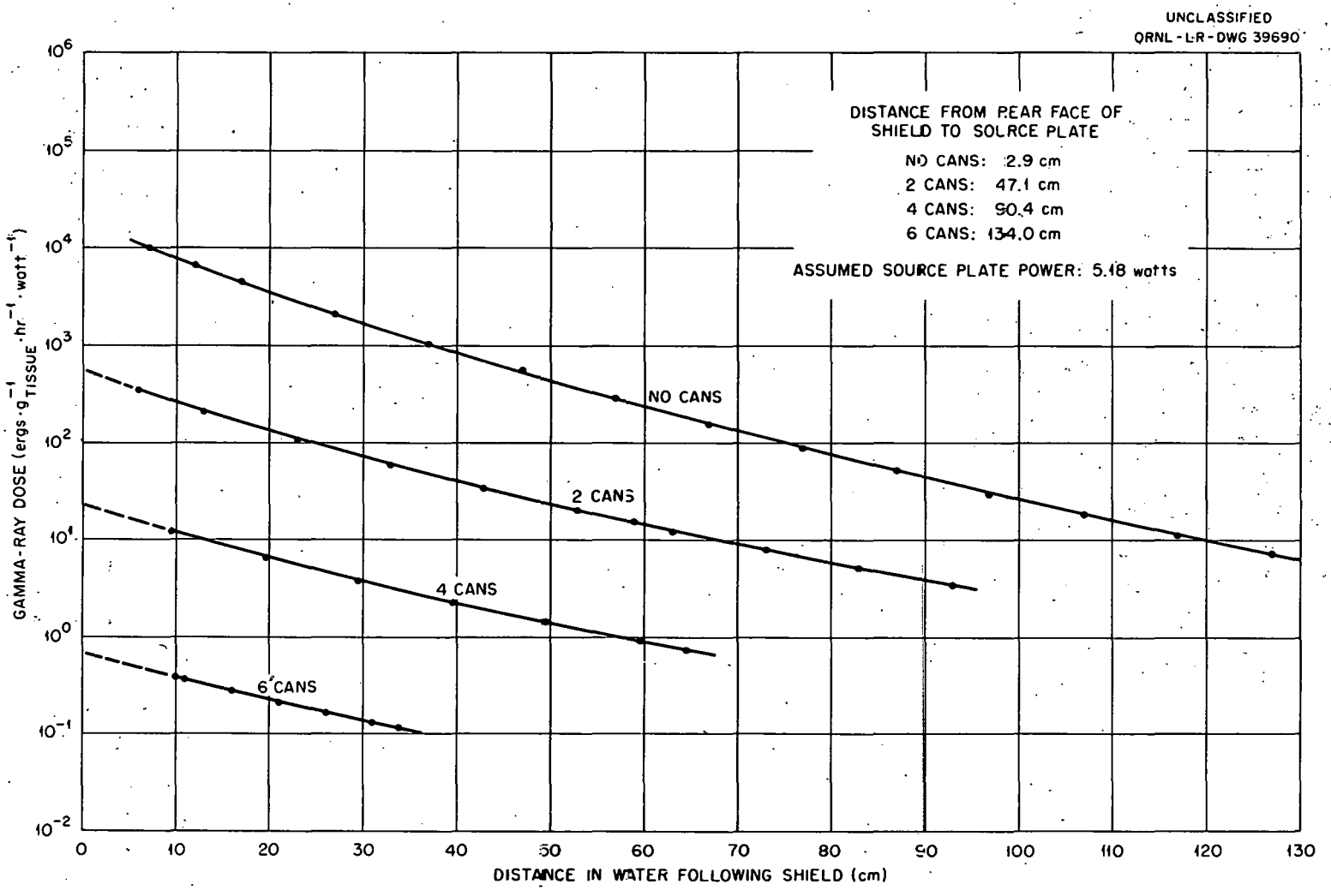

Fig. 19. Gamma-Ray Dose in Water Following Cans of Barytes Aggregate.

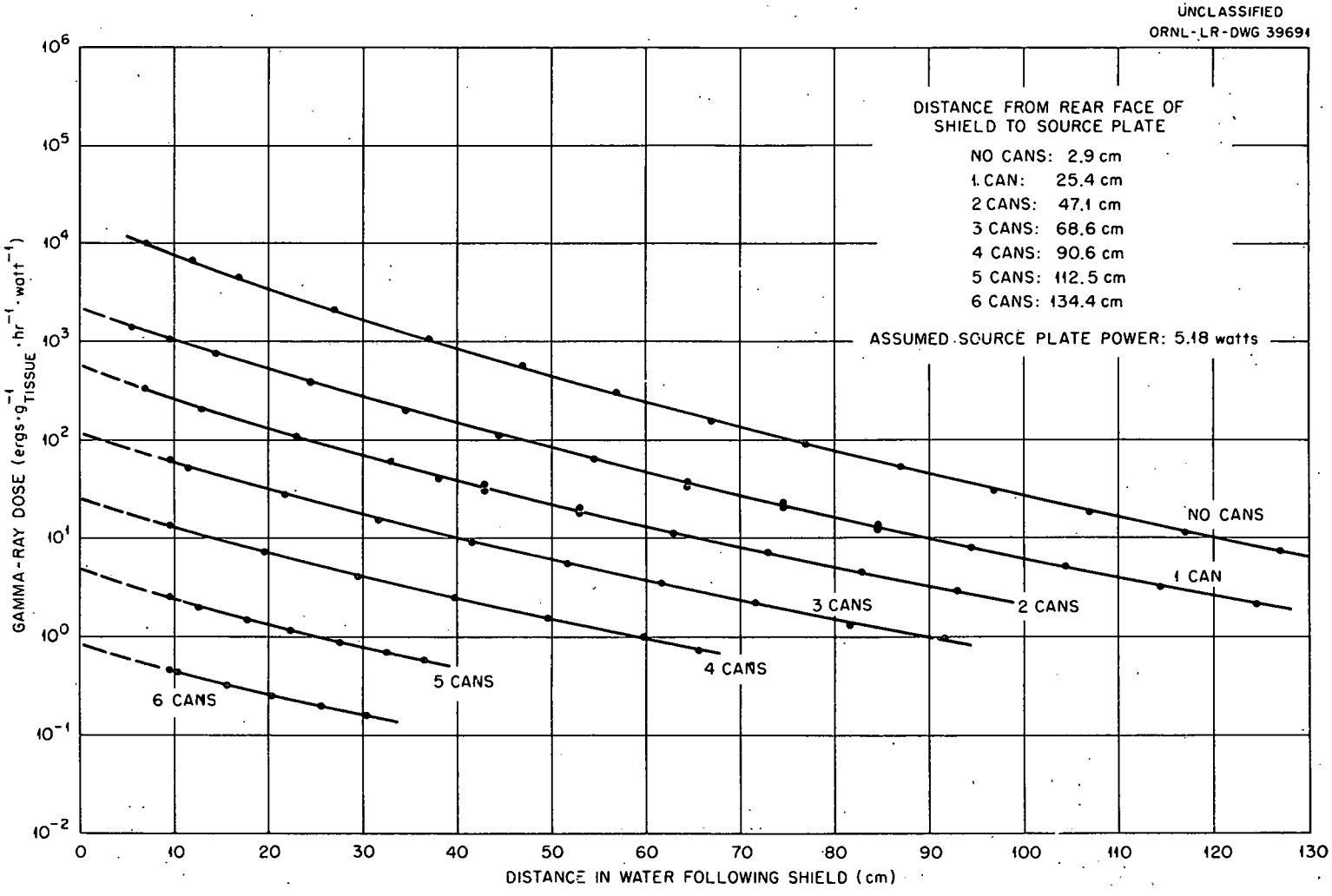

Fig. 2C. Gamma-Ray Dose in Water Following Cans of Barytes Aggregate Plus Cement.

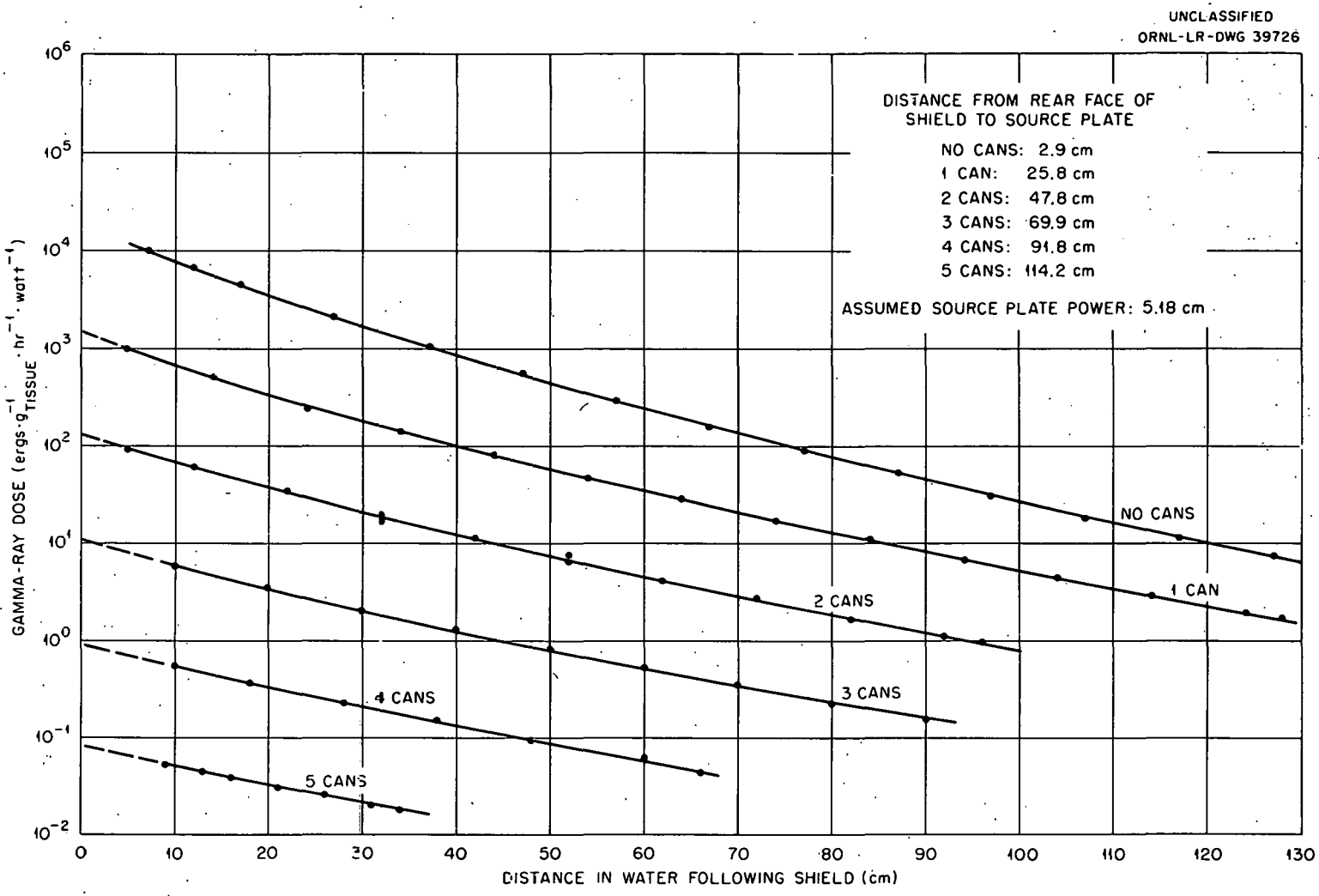

Fig. 21. Gamma-Ray Dose in Water Following Cans of Barytes Concrete.

Fast-neutron dose rates behind various test shields are shown in Figs. 16, 17, and 18. The detectors used for measuring this quantity are presumed to have a threshold at 200 kev. The dose rates ($ergs.g^{-1}.hr^{-1}$) are for tissue.

Figure 19, 20, and 21 show the gamma-ray dose rates measured behind various test shields. Here again the dose rates indicated are for tissue.

Interpretation of Results

It was noted previously that the hydrogen removal cross section decreases rapidly as neutron energy increases in the energy range of fast neutrons. The same is obviously true for water, since the cross section for hydrogen is the major contribution to the removal cross section. In a water medium, therefore, the fast neutrons existing at relatively large distances from a source, say 100 cm, can be presumed to have accomplished most of the penetration at high energy. This phenomenon has been thoroughly studied and forms the basis for calculating fast-neutron removal cross sections from measured data. It is generally accepted that the fast neutrons from a fission spectrum which have penetrated 100 cm of water were born in the vicinity of 8 Mev.[13]

The calculation of a removal cross section for a shield involves an analysis of the thermal-neutron flux in a water medium following the shield. The use of fast-neutron dose-rate measurements is not advantageous because lack of sensitivity of the detector prevents measurement of the dose out to large enough distances.

The analysis of the thermal-neutron flux to determine fast-neutron removal cross sections is based on the following argument. The thermal neutrons existint at a point in a water medium were in general born in the same vicinity,

---

13. H. Goldstein, Fundamental Aspects of Reactor Shielding (Reading: Addison-Wesley Publishing Co., Inc., 1959).

since the average diffusion length of a thermal neutron, the probable distance a thermal neutron travels before it is captured, is only about 2.9 cm for a water medium. The thermal-neutron flux at a given point then must be proportional to the flux of fast neutrons in the same vicinity. Evaluation of the proportionality is unnecessary, because the removal cross section is a function of the change in flux at a given water distance due to an added increment of shield.

Because of differences in density, it is usually convenient to compare the attenuation efficiencies by means of another parameter, the removal mass-attenuation coefficient. This is simply the removal cross section divided by the density ρ. Because Σ_R/ρ is thus essentially independent of density, it provides a more reasonable basis for comparisons of atomic properties.

The formula derived for the analysis of LTSF data[14,15] was used to compute several fast-neutron removal cross sections from the data of the present experiment. The complexity of the formula is the result of necessary geometric corrections due to the finite disk source. Since it involves several approximations, it is valid only for great distances, approximately 100 cm, from the source plate. The formula is as follows:

$$\frac{D_1(z)}{D_2(z+t)} = \frac{\lambda_1}{\lambda_2}\left(\frac{z+t}{z}\right)^2\left(1 - \frac{a^2 t}{4\lambda z(z+t) - a^2 z}\right) e^{-\Sigma_R t}$$

where

$D_1(z), D_2(z+t)$ = fluxes measured without and with a shield interposed, at distances z and z + t, respectively, in neutrons·cm^{-2}·sec^{-1}·w^{-1},

---

14. E. P. Blizard, Procedure for Obtaining Effective Removal Cross Sections from Lid Tank Data (Oak Ridge National Laboratory, 1954), ORNL-CF-54-6-164.
15. G. T. Chapman and C. L. Storrs, Effective Removal Cross Sections for Shielding (Oak Ridge National Laboratory, 1955), ORNL-1843.

λ_1, λ_2 = relaxation lengths in water, i.e., the distance that changes the flux by a factor of e, taken at the points where $D_1(z)$ and $D_2(z + t)$ are measured, respectively, cm,

λ = average relaxation length, cm (the arithmetic mean of λ_1 and λ_2),

a = source plate radius,
= 35.56 cm,

t = total thickness of shield interposed, including aluminum thicknesses, cm,

Σ_R = effective removal cross section for all material interposed, cm^{-1}.

The value of $\Sigma_R t$ thus determined has to be corrected to obtain the removal cross section for the material under consideration. The correction is merely the subtraction of the total aluminum thickness times the aluminum removal cross section, taken here to be 7.88×10^{-2} cm^{-1} (Ref. 15).

Fast-neutron removal cross sections were determined for z = 100 cm for each of the shielding materials studied. The results of these calculations are shown in Table 3. As mentioned previously, it is more convenient to compare removal mass-attenuation coefficients because of the differences in densities. These are also shown in Table 3.

Table 3. Measured Fast-Neutron Removal Cross Sections and Mass Attenuation Coefficients for Barytes Concrete Components

Material	Σ_R (cm^{-1})	Σ_R/ρ (cm^2/g)
Aggregate (ρ = 2.68 g/cm^3)	0.0662	0.0247
Aggregate and cement (ρ = 2.67 g/cm^3)	0.0633	0.0245
Concrete (ρ = 3.30 g/cm^3)	0.0993	0.0301

Table 4 gives an estimated removal mass-attenuation coefficient for barytes aggregate; Table 5 gives an estimated coefficient for cement. These calculations are included for comparison only since the weight percentages are estimated and many of the Σ_R/ρ values are interpolations from a small graph.[16] The fact that the estimates are close to the measured values, however, encourages belief that the test results are reasonable. It should be noted here that this approach, i.e., the estimation of the removal mass-attenuation coefficient for fast neutrons, can be used as a guide in selecting an aggregate for a neutron shield. Table 6 gives an estimated removal mass-attenuation coefficient based on chemical analysis of the barytes concrete. The results here should verify this technique as an expedient method for estimating removal mass-attenuation coefficients for concrete.

Table 4. Estimation of Removal Mass-Attenuation Coefficient for Barytes Aggregate

Compound	Σ_R/ρ (cm^2/g)[a]	Weight (per cent)	Weighted Σ_R/ρ (cm^2/g)
$BaSO_4$	0.0213	65.9	0.0140
SiO_2	0.0335	32.4	0.0108
H_2O	0.1000	1.7	0.0017
		Σ_R/ρ, total =	0.0265

a. G. T. Chapman and C. L. Storrs, Effective Removal Cross Sections for Shielding (Oak Ridge National Laboratory, 1955), ORNL-1845.

16. E. P. Blizard, "Nuclear Radiation Shielding," Nuclear Engineering Handbook, ed. by N. Etherington (New York: McGraw-Hill Book Co., Inc., 1958), p. 7-60.

Table 5. Estimation of Removal Mass-Attenuation Coefficient Type-I Portland Cement

Element	Σ_R/ρ $(cm^2/g)^{a,b}$	Weight (per cent)	Weighted Σ_R/ρ (cm^2/g)
Ca	0.024	47.9	0.0115
O	0.0372	35.3	0.0131
Si	0.0295	9.7	0.0029
Al	0.0292	3.1	0.0009
Fe	0.0214	1.8	0.0004
Mg	0.032	1.8	0.0006
S	0.0275	0.4	0.0001
		Σ_R/ρ, total =	0.0295

a. G. T. Chapman and C. L. Storrs, Effective Removal Cross Sections for Shielding (Oak Ridge National Laboratory, 1955), ORNL-1843.

b. E. P. Blizard, "Nuclear Radiation Shielding," Nuclear Engineering Handbook, ed. by H. Etherington (New York) McGraw-Hill Book Co., Inc., 1958, p. 7-60.

As another verification of the validity of the test results, the difference between the removal mass-attenuation coefficients for barytes and concrete and barytes-plus-cement can be reasonably accounted for by the difference in water content. The additional water, including water of hydration, amounted to 8.64 per cent of the total weight.

It was implied previously that the neutrons which have penetrated only a few centimeters of water are on the average much softer than those far out. A removal cross section taken at z = 20 cm should, therefore, be descriptive of an intermediate-energy component. If an intermediate-energy component has a removal cross section at least as large as the fast-neutron removal cross section measured far out, the moderation of intermediate-energy neutrons would presumably be satisfactory.

Table 6. Calculated Mass-Attenuation Coefficient for Barytes Concrete, with Chemical Analysis and Mass Attenuation Coefficients of Constituents

Constituent	Content (wt%)[a]	Σ_R/ρ (cm^2/g)[b]	Weighted Σ_R/ρ (cm^2/g)
Ba	36.4	0.0124	0.0045
S	8.7	0.0275	0.0024
O	27.8	0.0372	0.0103
Si	4.2	0.0295	0.0012
Ca	4.1	0.024	0.0010
Al	0.2	0.0292	0.0001
Fe	8.4	0.0214	0.0018
Mg	0.3	0.030	0.0001
H_2O	9.9	0.100	0.0099
		Σ_R/ρ, total =	0.0313

a. Normalized to 100 wt%; actual total from chemical analysis, 101 wt%.

b. From G. T. Chapman and C. L. Storrs, Effective Neutron Removal Cross Sections for Shielding, ORNL-1843 (1955); see also E. P. Blizard, Nuclear Engineering Handbook, ed. by H. Etherington, p. 7-60, McGraw-Hill, New York, 1958.

The determination of an intermediate-energy removal cross section involves a revision of the previously-stated removal cross section formula since the criterion that the distance be large, to keep λ_1 approximately equal to λ_2, is no longer satisfied. The revised formula for 20 cm of water is as follows:[9]

$$\frac{D_1}{D_2} = \frac{\lambda_1}{\lambda_2}\left(\frac{t_2}{t}\right)^2 \left(1 - \frac{a^2\Delta t}{4\lambda t_1 t_2 - a^2 t_1}\right) e^{-\Sigma_R \Delta t}$$

where

t_1 = specific thickness of shield, plus 20 cm,

Δt = added increment of shield, cm,

$t_2 = t_1 + \Delta t$, cm.

All other terms are the same as in the previous case.

The following intermediate-energy removal cross sections were determined from the measured data:

Barytes aggregate, $\Sigma_R = 0.0736$ cm^{-1}.

Barytes aggregate plus cement, $\Sigma_R = 0.0785$ cm^{-1}.

Barytes concrete, $\Sigma_R = 0.110$ cm^{-1}.

It will be noted that in all three cases intermediate-energy neutrons appear to be attenuated more efficiently than the very fast neutrons. Generally, this evidence would be sufficient indication that moderation is satisfactory in the epithermal region. A study of the fast-neutron dose-rate measurements, which can be extrapolated to zero water distance, will, however, reveal apparently contradictory information. The slope of the dose-rate curve behind four or five cans of barytes-plus-cement is steeper than for the same number of cans of barytes concrete. The steeper slope normally implies that the neutrons present have a lower average energy. Neutrons in the lower end of the intermediate-energy range are possibly not being attenuated as efficiently as was at first presumed. This effect seems slight, however, and it is therefore concluded that no serious low energy buildup occurred in any of the shields studied. The buildup of intermediate-energy neutrons may become more pronounced, however, in instances where the moisture in the aggregate is also removed.

With regard to proportioning, it is concluded that the barytes aggregate is a good aggregate for a neutron shield. The fast-neutron removal cross section of the aggregate, actual density considered, roughly matches that of water. In addition, it has no serious low points[17] in the cross sections for lower energies. Slight reductions in water content in order to obtain greater densities are therefore justifiable.

The fast-neutron dose rate measurements are shown in Figs. 16, 17, and 18. At large distances the fast-neutron removal cross section may be used to predict the dose rates shown in Fig. 22. It should be noted that these dose rates do not include the dose rates from thermal and epithermal neutrons. Although the dose rates from these low-energy neutrons may be small, they must be considered in shield design.

Figure 23 compares the gamma-ray dose rate behind various thicknesses of barytes concrete with that behind similar thicknesses of barytes aggregate and of barytes aggregate plus cement. The latter two curves are identical. The barytes concrete appears to be nearly 50 per cent more effective for gamma rays than are the aggregates alone.

In contrast to the relatively simple methods available, through use of the removal cross section concept, for the calculation of neutron penetration of concrete shields, the calculation of the gamma-ray dose rate to be expected behind a thick concrete shield is extremely complicated. The difficulty is due to the fact that the emergent gamma-ray dose consists largely of gamma rays produced either by neutron captures by shield nuclei or by inelastic scattering of neutrons within the shield. Capture gamma-ray energies range from ~ 2 to ~ 10 Mev, while the range of inelastic-scattering gamma-ray energies lies between 1 and 2 Mev. Thus sources of high-energy gamma rays are distributed throughout the thickness of the shield, and some

17. D. J. Hughes and J. A. Harvey, Neutron Cross Sections (Brookhaven National Laboratory Report w/addendum, 1955), BNL-325.

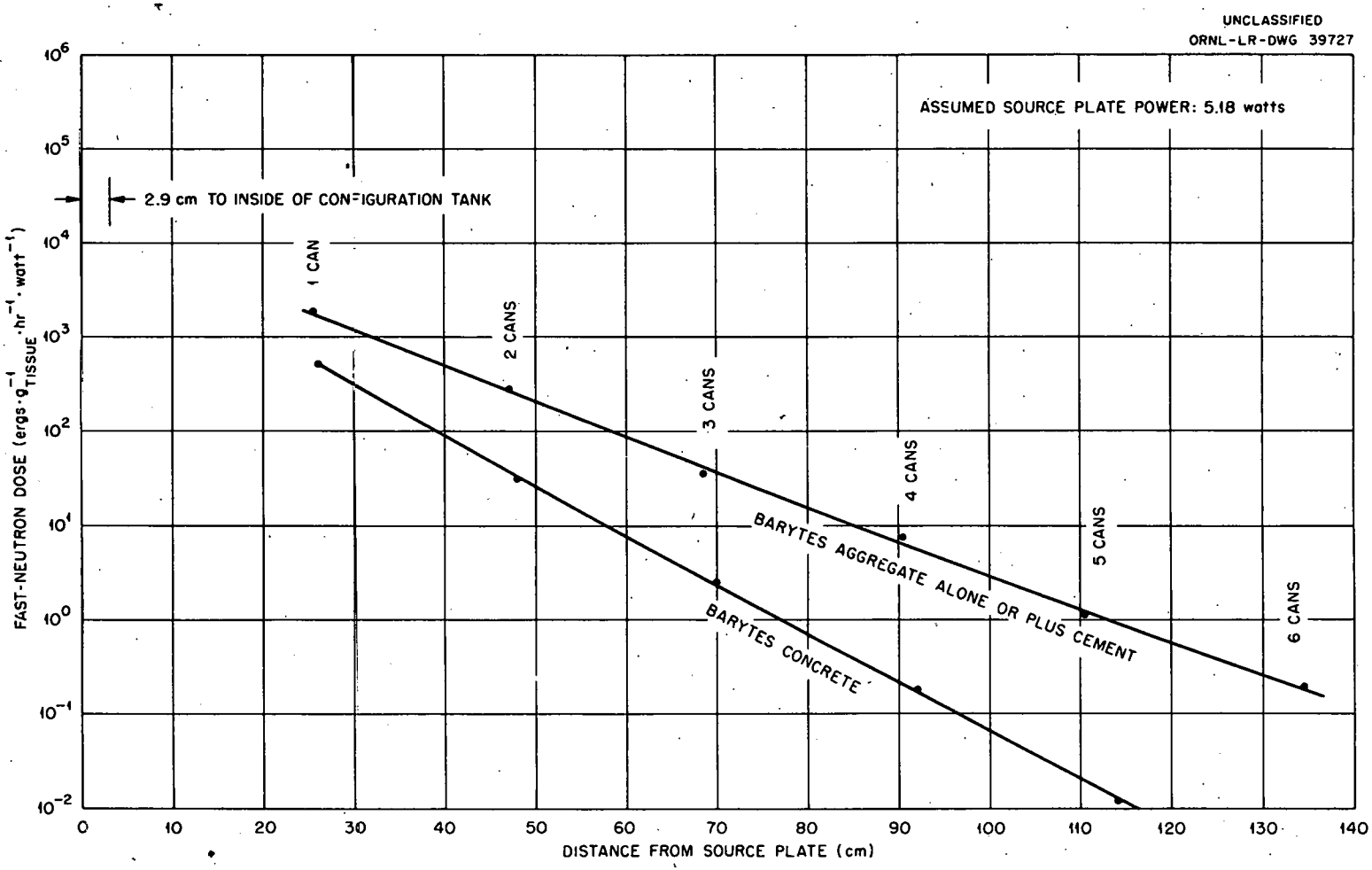

Fig. 22. Fast-Neutron Dose vs. Shield Thickness.

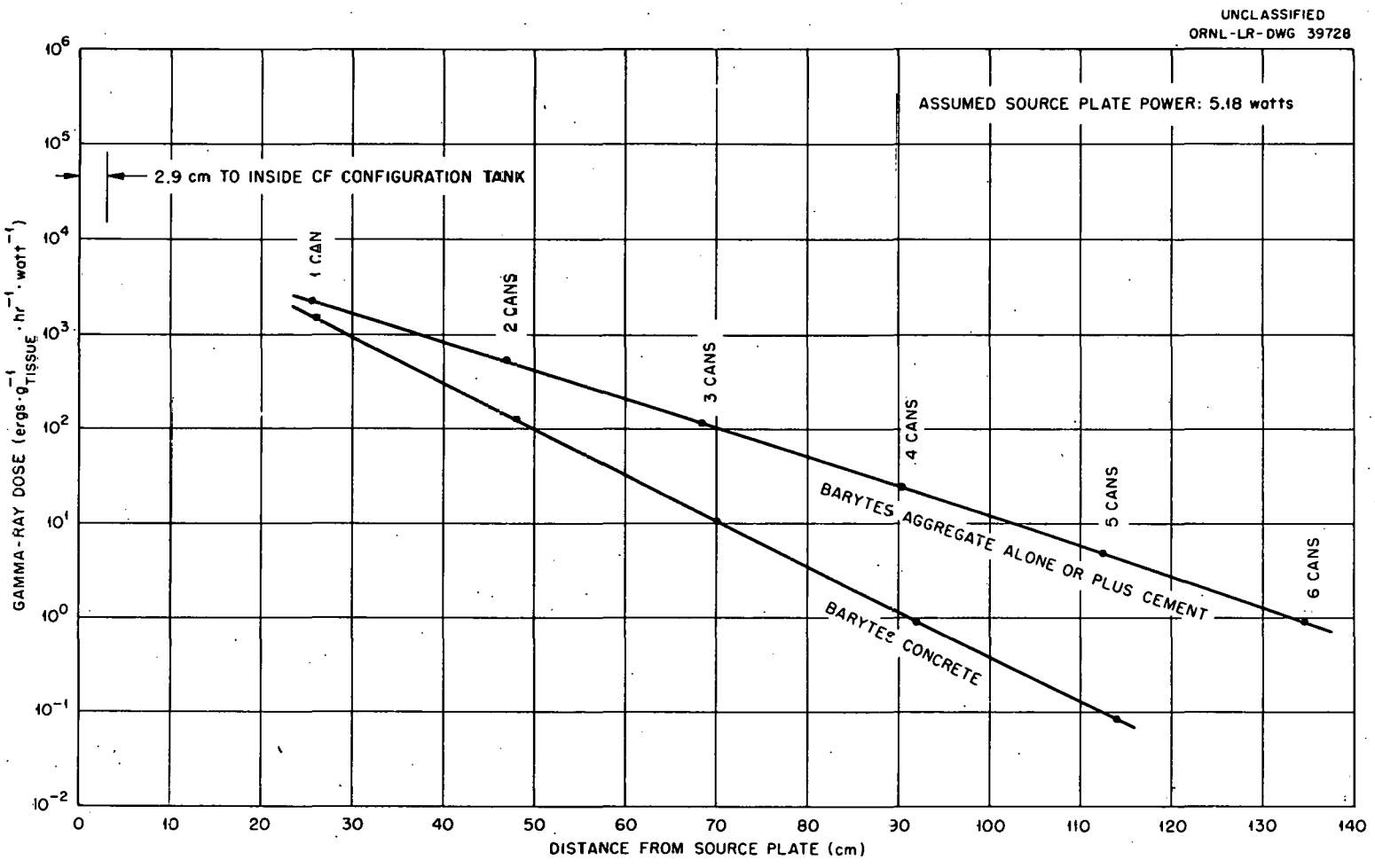

Fig. 23. Gamma-Ray Dose vs. Shield Thickness.

must lie very close to the outside surface of the shield. It has been suggested[18] that the inclusion of even small quantities of boron or lithium compounds in the concrete mix might noticeably reduce the number of capture gamma rays produced within the shield. Boron and lithium have high thermal-neutron capture cross sections, but on capturing a neutron emit easily stopped alpha particles rather than a high-energy gamma ray. (Boron, in addition to an alpha particle, gives a single 0.48-Mev gamma ray in ~ 93 per cent of absorptions, but these are usually quickly absorbed.)

CONCLUSIONS

The design of any structure as complex in function as a concrete radiation shield is, of necessity, fraught with compromise. The often-conflicting requirements of structural stability, high density, and large fast-neutron removal cross section, must be nicely balanced against cost, availability of materials, and protection against generation of excessive numbers of capture gamma rays.

The criteria developed in Section 1 of this paper serve usefully in the design of high-density concrete, of primary value in the shielding of gamma rays. If, in addition, a judicious selection of aggregate be made, ideally such that the aggregate chosen will have a fast-neutron removal cross section approaching that of water, then the criteria may apply equally well to the shielding of neutrons. The importance of capture gamma-ray sources cannot be overstressed. Their existence must be considered during all processes of aggregate selection, etc. If other considerations, in particular structural needs, permit use of capture-gamma-ray suppressing agents such as boron within the mix, then the lowered gamma-ray intensity may permit decreases in density that could result in more efficient neutron attenuation.

In the design of shields for high-temperature applications, similar basic considerations apply. Shields intended to withstand temperatures in the vicinity of 100°C may be improved by the use of hydrated lime as an admixture. Hydrated lime, often added to concrete to increase workability,

18. H. E. Banta and G. W. Leddicotte, Control of Gamma Radiation in Heavily Shielded Target Rooms, paper presented at the meeting of the Southeastern Section of the American Physical Society, Gatlinburg, Tenn., April 7-9, 1960.

contains approximately 25 per cent water by weight.[19] In this temperature range, a neutron shield may also be improved by employing a mix richer in cement. Although this may decrease gamma-ray attenuation efficiency, the total dose rate from neutrons and gamma rays may be reduced. Consideration may also be given to specific aggregates containing water-of-crystallization, such as limonite or serpentine. Studies recently concluded at Hanford[20,21,22,23] are expected to offer further insight into high-temperature shielding problems.

19. E. E. Bauer, Plain Concrete, McGraw-Hill Book Co., Inc., New York, 1949.

20. D. W. Wood, The Effect of Temperature on the Neutron Attenuation of Magnetite Concrete, HW-58497, Hanford Atomic Productc Operation (1958).

21. W. L. Bunch, Attenuation Properties of High Density Portland Cement Concretes as a Function of Temperature, HW-5456, Hanford Atomic Products Operation (1958).

22. E. G. Peterson, Shielding Properties of Ferrophosphorous Concrete as a Function of Temperature, HW-64774, Hanford Atomic Products Operation (1960).

23. E. G. Peterson, Shielding Properties of Ordinary Concrete as a Function of Temperature, HW-65572, Hanford Atomic Products Operation (1960).

ACKNOWLEDGEMENTS

Research conducted at the Oak Ridge National Laboratory was performed under an Atomic Energy Commission Fellowship administered by the Oak Ridge Institute of Nuclear Studies; to these institutions the author is indeed grateful. The author is also gratefully indebted to the Nuclear Engineering Department of the University of Florida for their sponsorship of a portion of the research.

For their encouragement and criticisms, the author wishes to express gratitude to the following: Professors R. W. Kluge, B. D. Spangler, and J. H. Schmertmann of the Civil Engineering Department, University of Florida; Professor W. F. Fagen of the Nuclear Engineering Department and Electrical Engineering Department, University of Florida; Mr. E. P. Blizard, Director, Neutron Physics Division, Oak Ridge National Laboratory; and Dr. Walter Zobel, leader, Lid Tank Shielding Facility, Oak Ridge National Laboratory.

Gratitude is expressed to other members of the Lid Tank Shielding Facility: J. M. Miller, Lincoln Jung, J. R. Taylor, Everett Beckham, and P. T. Perdue.